HHS Public Access

Author manuscript

Cell Rep. Author manuscript; available in PMC 2021 May 13.

Published in final edited form as:

Cell Rep. 2021 April 20; 35(3): 108992. doi:10.1016/j.celrep.2021.108992.

Glucose-mediated proliferation of a gut commensal bacterium promotes *Plasmodium* infection by increasing mosquito midgut pH

Mengfei Wang[#1,2], **Yanpeng An**[#1,3], **Li Gao**[#1,2], **Shengzhang Dong**[4], **Xiaofeng Zhou**[5], **Yuebiao Feng**[1,2], **Penghua Wang**[6], **George Dimopoulos**[4], **Huiru Tang**[1,3,*], **Jingwen Wang**[1,2,8,*]

[1]State Key Laboratory of Genetic Engineering, School of Life Sciences, Fudan University, Shanghai 200438, PRC

[2]Ministry of Education Key Laboratory of Contemporary Anthropology, School of Life Sciences, Fudan University, Shanghai 200438, PRC

[3]State Key Laboratory of Genetic Engineering, Zhongshan Hospital and School of Life Sciences, Human Phenome Institute, Metabonomics and Systems Biology Laboratory at Shanghai International Centre for Molecular Phenomics, Fudan University, Shanghai 200438, PRC

[4]W. Harry Feinstone Department of Molecular Microbiology and Immunology, Bloomberg School of Public Health, Johns Hopkins University, Baltimore, MD 21205, USA

[5]Human Phenome Institute, Fudan University, Shanghai 200433, PRC

[6]Department of Immunology, School of Medicine, The University of Connecticut Health Center, Farmington, CT 06030, USA

[8]Lead contact

[#] These authors contributed equally to this work.

SUMMARY

Plant-nectar-derived sugar is the major energy source for mosquitoes, but its influence on vector competence for malaria parasites remains unclear. Here, we show that *Plasmodium berghei* infection of *Anopheles stephensi* results in global metabolome changes, with the most significant impact on glucose metabolism. Feeding on glucose or trehalose (the main hemolymph sugars) renders the mosquito more susceptible to *Plasmodium* infection by alkalizing the mosquito

[*]Correspondence: huiru_tang@fudan.edu.cn (H.T.), jingwenwang@fudan.edu.cn (J.W.).

AUTHOR CONTRIBUTIONS

Conceptualization, M.W. and J.W.; methodology, M.W., Y.A., L.G., Y.F., S.D., G.D., X.Z., H.T., and J.W.; investigation, M.W., Y.A., L.G., G.D., H.T., and J.W.; formal analysis, M.W., Y.A., L.G., X.Z., and S.D.; writing – original draft, M.W., Y.A., L.G., H.T., and J.W.; writing – review & editing, M.W., Y.A., L.G., P.W., G.D., H.T., and J.W.; visualization, M.W., Y.A., L.G., H. T., and J.W.; funding acquisition, J.W.; resources, J.W., supervision, G.D., H.T., and J.W.

SUPPLEMENTAL INFORMATION

Supplemental information can be found online at https://doi.org/10.1016/j.celrep.2021.108992.

DECLARATION OF INTERESTS

The authors declare no competing interests.

midgut. The glucose/trehalose diets promote proliferation of a commensal bacterium, *Asaia bogorensis*, that remodels glucose metabolism in a way that increases midgut pH, thereby promoting *Plasmodium* gametogenesis. We also demonstrate that the sugar composition from different natural plant nectars influences *A. bogorensis* growth, resulting in a greater permissiveness to *Plasmodium*. Altogether, our results demonstrate that dietary glucose is an important determinant of mosquito vector competency for *Plasmodium*, further highlighting a key role for mosquito-microbiota interactions in regulating the development of the malaria parasite.

In brief

Wang et al. show that glucose/trehalose supplementation promotes the expansion of a commensal bacterium *Asaia* that modulates glucose metabolism, resulting in an increase of mosquito midgut pH. The pH increase promotes *Plasmodium berghei* sexual development.

Graphical Abstract

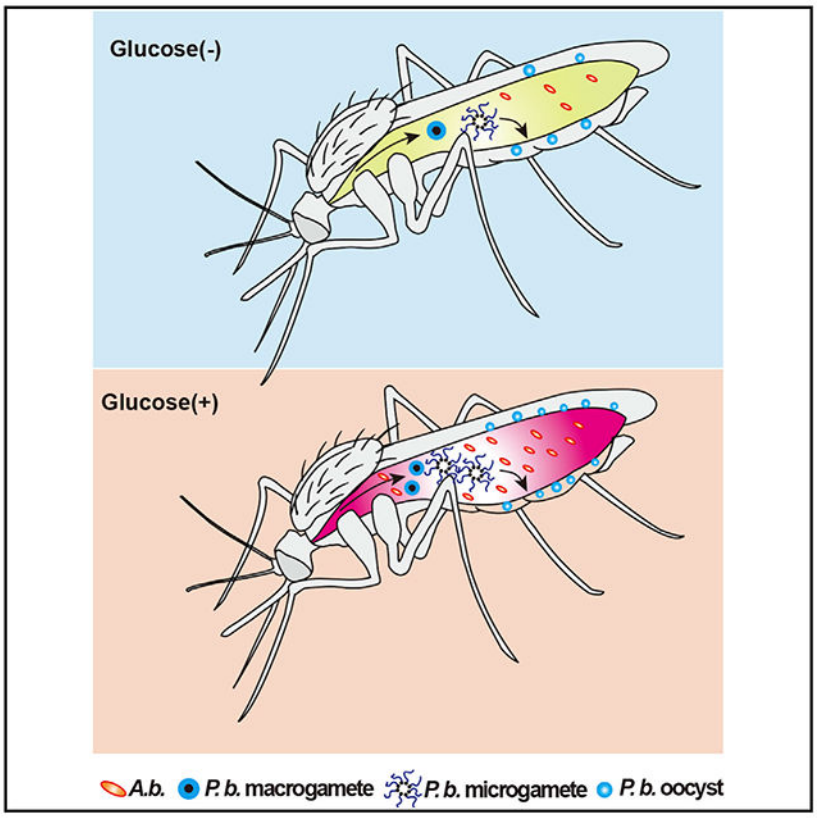

INTRODUCTION

Female mosquitoes require floral nectar and extra-floral plant fluids as energy sources. Sucrose and other sugars, including glucose, mannose, galactose, fructose, and gulose, are commonly present in plant nectar (Foster, 1995; Manda et al., 2007a, 2007b). These carbohydrates play important roles in influencing mosquito survival and fecundity (Manda et al., 2007a). Some indirect evidence also suggests that carbohydrate metabolism influences

the capability of mosquitoes to transmit malaria parasites. Trehalose, composed of two molecules of glucose, is the major hemolymph (blood) sugar and is utilized after being catabolized to glucose in insects (Becker et al., 1996). A reduction of trehalose level by knocking down the trehalose transporter AgTret1 impairs *Plasmodium falciparum* infection (Liu et al., 2013). Insulin/insulin-like growth factor signaling (IIS) is involved in regulation of *P. falciparum* infection in mosquitoes (Corby-Harris et al., 2010; Luckhart et al., 2013; Pietri et al., 2016). The knockdown of two insulin-like peptides, ILP3 and ILP4, increases *Anopheles* resistance to *P. falciparum* (Pietri et al., 2015). Ingestion of human insulin facilitates *P. falciparum* infection by inhibiting mosquito immune responses (Pakpour et al., 2012). Thus, glucose metabolism is expected to play a role in regulating *Plasmodium* infection in mosquitoes. However, the underlying mechanism remains unclear.

As an obligate intracellular parasite, *Plasmodium* can sense nutrient levels of mammalian hosts and obtain those nutrients to support growth and development (Mancio-Silva et al., 2017). Glucose is the primary energy source for the extensive proliferation of malarial parasites during both the liver and the blood stages (Jacot et al., 2016; Kirk, 2001; Olszewski and Llinás, 2011). *Plasmodium* infection of hepatic cells leads to a significant increase in glucose uptake (Meireles et al., 2017). Erythrocytes infected with *Plasmodium* utilize glucose up to 100 times faster than uninfected cells (McKee et al., 1946; Meireles et al., 2017; Roth, 1987). Inhibition of glucose uptake during either parasitic stage impairs the infection ability and attenuates virulence (Itani et al., 2014; Joët et al., 2003; Meireles et al., 2017; Saliba et al., 2004; Slavic et al., 2011). Different from the asexual-stage parasites that rely heavily on glucose fermentation for energy provision, the sexual development of *Plasmodium* in mosquitoes switches to a more efficient tricarboxylic acid (TCA) cycle for ATP production (Jacot et al., 2016). The increased reliance on the TCA is associated with increased glucose uptake and catabolism. Perturbation of TCA metabolism of parasites at this stage results in developmental arrest and death (Jacot et al., 2016). Thus, glucose metabolism in mosquitoes might play a role in influencing *Plasmodium* infectivity.

In addition to hosting malaria parasites, *Anopheles* mosquitoes are colonized by a broad spectrum of microbes that are critical for a variety of physiological functions, especially nutrient assimilation. Elimination of gut microbiota by antibiotics slows down food digestion (Gaio et al., 2011). *Serratia* sp. produces hemolysins that appear to facilitate blood digestion in *Anopheles* mosquitoes (Chen et al., 2017). *Acinetobacter* is able to digest blood containing α-keto-valeric acid, glycine, and nectar containing 4-hydroxy-benzoic acid and xylose (Minard et al., 2013). *Asaia bogorensis* has a functional nitrogenase that has been proposed to be responsible for the nitrogen metabolism in mosquitoes (Samaddar et al., 2011). In addition, the gut microbiota influence pathogen infection through directly secreting anti-pathogen molecules and stimulating the basal immune responses (Bahia et al., 2014; Cirimotich et al., 2011; Gonzalez-Ceron et al., 2003; Pumpuni et al., 1996). However, little is known about the carbohydrate metabolic interactions between *Anopheles* and gut microbiota or about the influence of such interactions on mosquito vector competence.

In this study, we use metabolomic analyses to show that *Plasmodium* infection increases glucose metabolism in *An. stephensi*. Oral administration of glucose and trehalose promotes *Plasmodium* infection. These interactions rely on the presence of the gut microbiota.

Glucose supplementation promotes the expansion of gut commensal bacterium *A. bogorensis*, which in turn modulates glucose metabolism, resulting in a raise in pH of the mosquito midgut. The midgut pH increase promotes *P. berghei* sexual development. We further explore the potential correlation between the abundance of *A. bogorensis* and the capacity of *An. stephensi* to transmit *Plasmodium* by providing mosquitoes with sugar meals simulating the sugar composition of floral nectar in a malaria-endemic area. Collectively, our results demonstrate that *A. bogorensis* participates in the glucose metabolism in *An. stephensi* and that this interplay influences the outcome of parasite infections.

RESULTS

P. berghei infection reduces glucose and trehalose levels in *An. stephensi*

To determine whether *Plasmodium* infection influences mosquito metabolism, we analyzed the metabolomic changes of whole *An. stephensi* at 1 day post-*P. berghei* infection (1 dpi) using nuclear magnetic resonance (NMR) spectroscopy. This is the stage when ookinetes invade midgut epithelium and elicit a global change in gene expression (Domingos et al., 2017; Dong et al., 2006). *P. berghei* infection induced profound metabolic changes in *An. stephensi*. In total, 21 metabolites showed differential abundances between infected and non-infected mosquitoes (Figure 1; Table S1). Among these were the metabolites associated with glucose metabolism such as trehalose, glucose, succinate, and citrate that were significantly reduced 1 dpi, while the abundances of pyruvate and acetate were significantly increased (Figure 1B). To examine whether the reduction of glucose could be due to differences in the blood that the mosquitoes had ingested, we compared the daily blood glucose levels in mice with and without parasite infection from 0 to 7 dpi. No significant differences in glucose levels were observed until parasitemia reached approximately 15% at 5 dpi. This was much higher than the parasitemia (6%) we used for mosquito metabolome analysis (Figure S1). Thus, these data suggest that *Plasmodium* invasion disrupts the homeostasis of glucose metabolism in *An. stephensi*.

We next specifically examined the total glucose and trehalose levels in the midgut tissue in which *Plasmodium* undergoes major developmental transitions, including gametogenesis, fertilization, and ookinete formation (Angrisano et al., 2012). Similarly, *P. berghei* infection was associated with significant decreases in total glucose and trehalose levels in the midgut at 1 dpi of infected blood (Figure 1C). Because the mosquito midgut is in constant association with commensal bacteria, to determine whether the gut microbiota may play a role in the observed sugar reduction during *Plasmodium* infection, we also measured the total glucose and trehalose levels in midguts of mosquitoes treated with a cocktail of antibiotics. Interestingly, when the majority of gut microbiota were removed, *P. berghei* infection did not result in decreases of the total glucose or trehalose levels in the midgut (Figure 1C). These results indicate that the gut microbiota contribute to the *Plasmodium*-mediated alteration of glucose metabolism in mosquitoes.

Increasing uptake of glucose/trehalose promotes *Plasmodium* midgut infection in *An. stephensi*

To examine the influence of glucose and trehalose on *Plasmodium* infection, we first maintained newly emerged mosquitoes on a 2% sucrose solution containing glucose (G), trehalose (T), or 10% sucrose (HS) for 5 days followed by feeding on *P. berghei*- and *P. falciparum*-infected blood (Figure 2A). The number of *P. berghei* oocysts increased significantly in the 0.1 M glucose and trehalose groups compared with the sucrose-only controls (S and HS) (Figures 2B and S2A). The 0.1 M trehalose group also showed an increased *P. falciparum* oocyst intensity compared with the sucrose control (S) (Figure 2C). However, a simple increase of sucrose concentration failed to increase infection of either *P. berghei* or *P. falciparum* (Figures 2B, 2C, and S2B). Neither increased sucrose concentrations influenced mosquito blood intake or reproduction (Figures S2C and S2D). In the mosquitoes from which microbiota were removed by antibiotics treatments, sucrose concentration did not affect the *Plasmodium* infection outcome (Figure S2E). These results indicate that the sucrose levels (2%–10%) have little influence on mosquito physiology or *Plasmodium* infection. Oral administration of glucose (G) through the sugar diet to mosquitoes post-infectious blood (IB) meal had no influence on parasite infection (Figure S2F), suggesting that the metabolic changes (or mechanisms) by which glucose and trehalose influence *Plasmodium* infection are initiated prior to the formation of oocysts.

The *P. berghei* infection-mediated decrease of glucose and increase of pyruvate suggest that parasite invasion of the midgut epithelium might increase glycolysis activity. We next fed the glycolysis inhibitor 2-deoxy-D-glucose (2-DG) together with glucose to mosquitoes prior to *Plasmodium* infection. Feeding on 2-DG completely abolished the effect of glucose on *P. berghei* infection, rescuing it to the control level (Figure 2D). However, mosquitoes administrated with 2-DG post-*P. berghei* infection showed no effect on parasite infectivity (Figure S2F). These results suggest that increasing glucose and trehalose uptake in *An. stephensi* before parasite infection promotes *Plasmodium* parasite infection.

Plasmodium relies on host glucose as an energy source (Olszewski and Llinás, 2011), so we next examined whether glucose-mediated enhancement of *P. berghei* infection could be due to the increased availability of sugar. The total trehalose + glucose level was examined in midguts and hemolymph 1 day prior to (−1 dpi) and post- (1 dpi) feeding on infected blood, respectively (Figure 2E). Increasing sugar uptake by feeding mosquitoes on G, T, and HS diets all significantly increased the sugar level in midguts and hemolymph before blood feeding (Figure 2E). Treatment with 2-DG also resulted in an increased total sugar level, especially in midguts prior to *Plasmodium* infection (Figure 2F). However, the increased sugar level in HS- and 2-DG-fed mosquitoes failed to increase *Plasmodium* infection intensity. Altogether, these data show that the glucose- and trehalose-mediated increases in susceptibility of *An. stephensi* to *Plasmodium* infection were not due to the elevated availability of glucose or trehalose in the mosquitoes.

Glucose/trehalose supplementation facilitates *P. berghei* infection by promoting proliferation of *Asaia bogorensis*

Several studies have shown that the mosquito gut microbiota influence vector competence for *Plasmodium* (Ricci et al., 2012). Inspired by our finding that *P. berghei*-induced reduction of total carbohydrates relies on the presence of the gut microbiota, we examined whether the microbiota were involved in the glucose-mediated modulation of parasite infection. Mosquitoes were fed with S and G supplemented with an antibiotics cocktail to suppress the gut microbiota prior to infection. Glucose supplementation led to a significant increase of *P. berghei* oocyst numbers in septic mosquitoes but failed to do so in the antibiotics-treated aseptic mosquitoes (Figure 3A). Aseptic *An. stephensi* had significantly higher sugar levels than those in the non-antibiotics-treated group, further confirming that gut microbiota are responsible for the sugar consumption (Figure S3A).

To identify the specific bacteria responsible for sugar catabolism, we analyzed the gut microbiota community structure present in mosquitoes that had fed on S and G using 16S rRNA pyrosequencing (Figures 3B and S3). A total of 729,898 reads with a median length of 415.9 bp were obtained, identifying 1,879 bacterial operational taxonomic units (OTUs). Principal-component analysis showed that gut microbiota of mosquitoes fed on the G diet clustered separately from those that fed on the S controls (Figure S3B). Glucose supplementation significantly increased the relative abundance of *Asaia sp*. in *An. stephensi* midgut compared with the S group (Figures 3B and S3C), and *Asaia bogorensis* was the bacterial species enriched by glucose diet in *An. stephensi*. The results of real-time quantitative PCR confirmed that supplementation of glucose and trehalose significantly increased the number of *A. bogorensis* (Figure 3C). Increased fluorescent signals were also observed in midguts of *An. stephesi* on the G diet, compared with controls, by fluorescent *in situ* hybridization (FISH) analysis (Figure 3D).

We next colonized antibiotics-treated mosquitoes with *A. bogorensis* and analyzed their susceptibility to *P. berghei* infection. Two dpi, *A. bogorensis* successfully colonized the midgut, as the abundance of this bacterium was significantly higher than that in aseptic mosquitoes (Figure S3D). Re-colonization of *A. bogorensis* alone was not able to change infection intensity compared with the antibiotics-treated cohort (Figure 3E). However, the addition of glucose significantly increased the median oocyst number from 32 to 61 in *A. bogorensis* mono-associated mosquitoes (Figure 3E). Moreover, colonization with *A. bogorensis* significantly reduced the midgut carbohydrate level (Figure S3E). Altogether, these data indicate that glucose and trehalose administration to mosquitoes promotes *A. bogorensis* proliferation in the midgut, and this expansion of *A. bogorensis* renders the mosquito more susceptible to parasite infection.

Glucose/trehalose promotes *P. berghei* infection by altering the midgut acid-base balance

To determine how glucose promotes *P. berghei* infection, we first performed an RNA sequencing (RNA-seq)-based transcriptomic comparison between *An. stephensi* midguts fed on S and G at −1 and 1 dpi. A total of 460 and 97 genes were differentially expressed at −1 dpi and 1 dpi, respectively (Table S2). Supplementation of glucose significantly upregulated the expression of genes associated with glucose and general sugar metabolism and transport

at −1 dpi. However, most of these genes were downregulated at 1 dpi (Figure 4A). Notably, glucose and trehalose supplementation significantly repressed the activity of Imd-pathway-associated genes (Figures 4A and S4A). The expression level of *caudal*, the negative regulator of the Imd pathway, was significantly upregulated, while the peptidoglycan recognition protein *pgrp-lc* and the antimicrobial peptides *defensin* and *cecropin* were significantly downregulated both prior to and after the IB meal (Cirimotich et al., 2010; Clayton et al., 2013, 2014; Song et al., 2018) (Figure 4A). It is possible that the increased susceptibility to *P. berghei* infection may have partly resulted from the downregulation of the immune deficiency (Imd) pathway. We next stimulated the expression of Rel2-regulated immune genes by knocking down *caudal*. Mosquitoes treated with double-stranded RNA targeting green fluorescent protein (dsGFP) were used as controls (Figure S4B). However, supplementing the sugar meal with glucose in these mosquitoes resulted in a similar increased susceptibility to infection compared with those on the S diet (Figure S4C). Neither did *caudal* silencing affect the abundance of *A. bogorensis* (Figure S4D). Thus, the Imd pathway did not seem to be exclusively responsible for the glucose-mediated increased permissiveness to *P. berghei* infection (Garver et al., 2009).

Moreover, we observed a group of genes encoding vacuolar ATPase (V-ATPase) subunits, such as *H_N1, _H_N2, _H_N3, _H_N4, _G1, _G2*, and *_C*, that were differentially regulated between the G and S cohorts at the two time points (Figure 4A). V-ATPase hydrolyzes ATP and transports protons across membranes. The enzyme is critical for controlling the intracellular and extracellular pH of cells (Boudko et al., 2001a; Hayek et al., 2019; Linser et al., 2009). To examine whether V-ATPase is responsible for the glucose-induced increase of vector competence, we impaired V-ATPase function by specifically knocking down a *V-ATPase* gene encoding cytoplasmic V1 domain subunit H *(V-ATPase_H_N3)* or through supplementation of the sugar meal with the V-ATPase inhibitor Bafilomycin A1 in normal S-fed mosquitoes (Figure 4B). Silencing this gene significantly increased oocyst number compared with dsGFP controls in mosquitoes fed on S (Figures 4C and S4E). Again, oral administration of Bafilomycin A1 to *An. stephensi* dramatically increased oocyst numbers of *P. berghei* compared with the untreated controls (Figure 4D) (Boudko et al., 2001b; Yoshimori et al., 1991). These results indicate that glucose-induced enhancement of *P. berghei* infection may be the result of a modulation of V-ATPase activity.

As V-ATPase is involved in maintaining acid-base balance in mosquito midguts (Jagadeshwaran et al., 2010; Patrick et al., 2006; Zhuang et al., 1999), we next examined whether disruption of V-ATPase expression could influence midgut pH. As expected, inhibition of V-ATPase activity, by either gene silencing or Bafilomycin A1 supplementation, increased midgut pH compared with controls, as shown by an *m*-Cresol purple pH staining assay (Figures 4E and 4F). Thus, these results indicate that inhibiting V-ATPase activity led to an increase in midgut pH.

We next examined whether glucose supplementation could influence midgut pH. Mosquitoes were fed with S, G, T, HS, or 2-DG for 5 days, and midguts were dissected for pH analysis (Figure 4G). Addition of glucose and trehalose significantly increased midgut pH compared with controls (Figure 4G). Inhibition of glycolysis by 2-DG restored the glucose-induced change in pH back to control levels (Figure 4G). Thus, our results show that administration

of glucose and trehalose dysregulates expression of V-ATPase that in turn is responsible for maintaining homeostasis of the midgut pH.

To examine whether elevated pH enhances *Plasmodium* infection, we next fed *An. stephensi* with 2% S containing different concentrations of $NaHCO_3$ (Figures 4H and S4F). Addition of 0.1 M $NaHCO_3$ dramatically increased midgut pH and significantly increased susceptibility to infection, as measured by increased oocyst numbers compared to control mosquitoes (Figures 4I, S4F, and S4G). In these mosquitoes, we also observed a significant reduction in Imd signaling activity both before and after *P. berghei* infection, suggesting that the downregulation of immune activity might be a result of an increase in pH (Figure S4H). To further validate that pH influences *Plasmodium* infection, we fed *An. stephensi* with multiple acids through the 2% sugar meal (Figure 4H) and found that acetic acid, lactic acid, and succinic acid acidified the midgut and significantly reduced oocyst number compared to controls (Figure 4J). Taken together, these findings suggest that glucose/trehalose administration in mosquitoes disturbs pH homeostasis in the midgut, which then facilitates *Plasmodium* infection.

A. bogorensis is responsible for glucose-/trehalose-mediated elevation of midgut pH

In light of our finding that glucose and trehalose supplementation promote proliferation of the gut commensal *A. bogorensis* and increase midgut pH, we were interested to know whether *A. bogorensis* could be responsible for controlling the midgut acid-base balance. The midgut pH levels of antibiotics-treated mosquitoes that were mono-colonized by *A. bogorensis* and fed on S and G were analyzed by *m*-Cresol purple dye. Antibiotics-treated mosquitoes on the same diet and *Enterobacter*-sp.-colonized mosquitoes were used as controls. Neither glucose diet nor re-colonization of *A. bogorensis* alone increased midgut pH (Figure 5A). Colonization of *Enterobacter* sp. that effectively inhibits *Plasmodium* infection did not affect midgut pH (Figures S4I and S4J) (Song et al., 2018). Only *A. bogorensis* recolonized antibiotics-treated mosquitoes fed with G had dramatically increased midgut pH compared with non-G-fed mosquitoes (Figure 5A). In combination with our previous finding that glucose selectively expands *A. bogorensis*, these results indicate that glucose catabolic activity of *A. bogorensis* might contribute to the pH changes in the mosquito midgut.

Because of technical difficulties in analyzing metabolites of *A. bogorensis* in the mosquito midgut, we compared sugar metabolites of conditioned media from *A. bogorensis* grown in the presence of 2% sucrose supplemented with either 0.1 M glucose or trehalose for 3 days using NMR analysis. Different sugar compositions did not influence the growth of *A. bogorensis* (Figure 5B). However, supplementation of glucose and trehalose significantly altered the levels of 15 metabolites, with two glucose metabolites–citrate and succinate–significantly reduced (Figure 5C; Table S3). The reduction of these acids might result in the increase of pH in the medium. We next examined pH of the conditioned medium and found that it was higher in glucose- and trehalose-supplemented media than that of sucrose-alone medium (Figure 5D). These data suggest that *A. bogorensis* is able to modulate its metabolic activities in response to different carbohydrates, leading to the alteration of the midgut pH.

Elevation of midgut pH promotes *P. berghei* gametogenesis

Plasmodium male gametogenesis is triggered by the pH increase as the parasite is passed from the mammalian host (pH = 7.2) to the mosquito midgut (pH = 8) (Bennink et al., 2016; Billker et al., 2000; Carter and Nijhout, 1977; Jiang et al., 2020; Kawamoto et al., 1991). Based on our finding that expansion of *A. bogorensis* increased the midgut pH, we hypothesized that this pH elevation could benefit *P. berghei* sexual development in the midgut. Gametes will develop around 15 min after *Plasmodium* is ingested into the mosquito midgut (Bennink et al., 2016). We first quantified the mRNA abundances of six *Plasmodium* genes associated with *Plasmodium* male gametogenesis in the midgut of *An. stephensi* fed on the four sugar diets–S, G, 2-DG, and HS–10 min post infection (Figure 6A). These genes were calcium-dependent protein kinase 1 (*cdpk1*), protein phosphatase 1 (*ppm1*), basal body protein SAS-6 (sas-6), the sexual stage-specific actin isoform actin 2 (*actin 2*), gamete egress and sporozoite traversal protein (*gest*), and male development gene-1 (*mdv-1*)(Billker et al., 2004; Deligianni et al., 2011; Guttery et al., 2014; Lanfrancotti et al., 2007; Marques et al., 2015; Olivieri et al., 2015; Ponzi et al., 2009; Sebastian et al., 2012; Sturm et al., 2015; Talman et al., 2011; Theriot et al., 2014; Yeoh et al., 2017; Yuda et al., 2015). As expected, five of the six genes (*cdpk1*, *ppm1, sas-6, gest*, and *mdv-1*) were significantly upregulated in midguts of glucose-fed mosquitoes, while feeding on either 2-DG or HS did not influence the expression levels of most of these genes (Figure 6A). We next analyzed the expression levels of the same six genes in midguts of *A. bogorensis*-recolonized *An. stephensi* fed on S and G 10 min post infection (Figure 6B). Colonization of *A. bogorensis* in glucose-fed mosquitoes significantly elevated expression of four of the six genes associated with microgamete development (Figure 6B). Similarly, the addition of $NaCHO_3$ induced the expression of most of these genes without changing *P. berghei* mitochondrial energy metabolism (Figure S5). To further confirm that an increase of pH promotes male gametogenesis, we visualized the exflagellation by staining the blood bolus from mosquito midguts using Giemsa staining. There was a significantly higher number of exflagellations and a higher exflagellation rate in G- and T-fed mosquitoes, respectively, than in S-fed mosquitoes (Figures 6C and 6D). These results suggest that elevated midgut pH upregulated expression of gametogenesis-related genes, thereby promoting male gamete formation in the midgut.

Sugar composition of natural plants influences the abundance of *A. bogorensis* and vector competence

Studies have shown that the diversity of natural plants affects the capacity of *Anopheles* mosquitoes to transmit *Plasmodium* parasites (Ebrahimi et al., 2018; Gu et al., 2011; Hien et al., 2016). We hypothesized that the sugar composition of different plant nectars might differentially promote *A. bogorensis* proliferation in a way that influences the vector competence of *Anopheles* mosquitoes. We compared the abundance of *A. bogorensis* in mosquitoes feeding on sugar meals simulating the nectar of five plants (*Tecoma stans, Senna didymobotrya, Ricinus communis, Parthenium hysterophorus*, and *Lantana camara*) found in western Kenya before a blood meal (Manda et al., 2007b) (Figure 7A). Flowers of *T. stans* and *S. didymobotrya* and leaves and stems of *R. communis* and *P. hysterophorus* are the favored sugar resources of *An. gambiae* in western Kenya, while plant sap of *L. camara* leaves and stems is the least preferred (Manda et al., 2007b). Sugar solutions based on the

composition and water content of five plant species were prepared according to established recipes (Abebe, 2015; Abere and Enoghama, 2015; Fatimah and Ahmad, 2009; Manda et al., 2007b; Sowmya et al., 2019) (Figure 7A). The *T. stans* and *S. didymobotrya* meals significantly increased the abundance of *A. bogorensis* as glucose did (Figure 7B). We next examined the susceptibility of these mosquitoes to *P. berghei* infection. As expected, mosquitoes in which *A. bogorensis* was expanded had significantly higher oocyst numbers compared with S controls (Figure 7D). The abundance of glucose was positively correlated with *A. bogorensis* number (Figure 7E) and oocyst number (Figure 7F) by variance analysis. Although *T. stans, S. didymobotrya, R. communis*, and *P. hysterophorus* are the four most favored plant species of *Anohpeles* mosquitoes, their ability to expand *A. bogorensis* varies. Those promoting proliferation of *A. bogorensis* also facilitate *Plasmodium* infection in mosquitoes.

DISCUSSION

Sugar is a major energy source for mosquitoes, but its influence on the capability of the mosquito to transmit pathogens remains unclear. In this study, we demonstrated that *Plasmodium* infection disrupts the homeostasis of glucose metabolism in *An. stephensi*. This disturbance relies on the presence of the commensal bacterium *A. bogorensis*. The proliferation of this bacterium changes glucose metabolism and increases pH in the midgut, thereby promoting *Plasmodium* gametogenesis and infection.

Unlike the rapid proliferation in the mammalian stage, *Plasmodium* undergoes a drastic reduction during the early stage of its infection in mosquitoes (Smith et al., 2014). Even reduced in number, *P. berghei* infection still elicits significant changes in *An. stephensi* metabolism, and in particular, the levels of glucose and trehalose become significantly reduced at 1 dpi. Here, we demonstrated that the glucose and trehalose reduction during *Plasmodium* infection is due to the presence of gut microbiota. The exponential proliferation of gut microbiota 24 h after blood feeding might modulate mosquito metabolism (Pumpuni et al., 1996; Wang et al., 2012), and this modulation might vary in response to *Plasmodium* infection. Although we demonstrated that the changes of glucose and trehalose in mosquitoes were not due to the changes of glucose in mouse plasma, we cannot exclude the possibility that the levels of other metabolites in mosquitoes might have been affected through ingestion of infectious mouse blood (Li et al., 2008). These metabolites might also play roles in regulating vector competence of mosquitoes. It would be interesting to investigate the influence of metabolites in mouse plasma on *Plasmodium* transmission from hosts to mosquitoes in the future.

Glucose is an important energy source for all living organisms (Yuval et al., 1994; Zielke et al., 1984). Trehalose is the major hemolymph sugar in insects, and it can be utilized after conversion to glucose (Becker et al., 1996). Our data show that trehalose supplementation increases both *P. berghei* and *P. falciparum* infections. However, glucose had no effect on *P. falciparum* infection. *P. falciparum* in this study was cultured *in vitro* in a blood medium differing substantially from that of human blood (Carter et al., 1993; LeRoux et al., 2009). Such a difference, especially in the increases of glucose concentration and pH in the medium, might influence *P. falciparum*, making it unresponsive to glucose treatment

(LeRoux et al., 2009). To simulate the *in vivo* infection process, we mostly used *P. berghei* that is naturally transmitted from mice to mosquitoes.

We next demonstrated that *A. bogorensis* participates in the regulation of midgut pH. *A. bogorensis* oxidizes acetate and lactate to carbon dioxide and water but does not oxidize ethanol to acetic acid (Yamada et al., 2000). Our metabolomics data show significant decreases of citrate and succinate in the conditioned media supplemented with glucose and trehalose. These results confirm that *A. bogorensis* has less capacity for acid production than other bacteria in the gut (Ano et al., 2008). This explains why expansion of *A. bogorensis* contributes to the increase of midgut pH in glucose- and trehalose-supplemented mosquitoes. However, the promotion of *A. bogorensis* proliferation by trehalose and glucose was not observed in antibiotics-treated mosquitoes recolonized with this bacterium. Similarly, the growth rates of *A. bogorensis* in S, T, and G media were comparable. One explanation is that other gut commensals might compete with *A. bogorensis* for carbon in mosquitoes on a sugar diet. When glucose or trehalose is added, *A. bogorensis* outcompetes other bacteria by taking advantage of the two carbohydrates. When *A. bogorensis* is the only bacterium present, its growth is not affected by glucose, trehalose, or sucrose, but its metabolism is differentially regulated. Another limitation here is that we have difficulty in detecting the metabolite changes in mosquito midguts due to the large amount of sample required for NMR. Further investigation is needed to examine the metabolite dynamics *in vivo* using other technology.

It is known that a pH increase triggers male gametogenesis *in vitro* (Billker et al., 1997; Jiang et al., 2020; Kawamoto, 1993). We demonstrated that the pH increase in the midgut promotes microgamete formation as expected. Consistent with our finding, acidification of tsetse fly midgut by colonization of a commensal bacterium of *An. gambiae* inhibits trypanosome infection (Weiss et al., 2019). A slightly alkaline condition increases Zika virus survival and infectivity and promotes its transmission from mammals to *Aedes* mosquitoes (Du et al., 2019).

Mosquitoes are able to differentiate between plant species (Gouagna et al., 2014; Manda et al., 2007a, 2007b). Feeding on the preferred plants increases their longevity and fecundity (Manda et al., 2007b; Stone et al., 2012; Yu et al., 2016). The sugars from different plant species also influence the capability of *Anopheles* to transmit malaria parasites (Ebrahimi et al., 2018; Gu et al., 2011; Hien et al., 2016). Although we have no access to the natural plants present in malaria-endemic areas, by using artificial sugar meals that have the same composition of the four most favored and one less favored plant saps as mosquito diets, we demonstrated that the sugar composition of plant sap determines the vector capacity through its ability to promote the proliferation of *A. bogorensis*. Notably, *P. hysterophorus* is an exception in that mosquitoes feed on it quite frequently, but with decreased longevity and fecundity (Manda et al., 2007a, 2007b). Neither does it promote *P. berghei* infection compared with other mosquito-preferred plants. Thus, *P. hysterophorus* might be an ideal plant species that could reduce the mosquito's malaria transmission potential. Further studies are needed to investigate the influence of natural plant saps on the composition of field *Anopheles* microbiota and to examine the influence of *A. bogorensis* from field mosquitoes on malaria parasite infection outcome.

In summary, our study provides crucial molecular insights into how a complex interplay between glucose metabolism of *An. stephensi* and a component of its gut microbiota, *A. bogorensis*, influences *Plasmodium* infection. Our work sheds new light on the mechanism of the gut microbiota in influencing mosquito metabolism and parasite infection. We also provide evidence that different sugar composition of plant saps may influence malaria transmission through a modulation of *A. bogorensis* proliferation. Thus, our work provides an important step toward a more comprehensive understanding of metabolic interactions among *Anopheles*, gut microbiota, and malaria parasites.

Limitations of the study

Our data demonstrate that glucose/trehalose supplementation promotes *Plasmodium* infection through increasing midgut pH. The gut microbiota, *A. bogorensis*, and mosquito V-ATPase are both responsible for regulating midgut pH. However, whether these two components work independently or collaboratively remains unknown. Further investigations will be needed to disentangle the interactions between V-ATPase and gut microbiota on midgut pH regulation.

STAR★METHODS

RESOURCE AVAILABILITY

Lead contact—Further information and requests for resources and reagents should be directed to and will be fulfilled by the lead contact, Jingwen Wang (jingwenwang@fudan.edu.cn).

Materials availability—This study did not generate new unique reagents.

Data and code availability—The published article includes all datasets generated or analyzed during this study.

The accession number for the raw RNA-Seq sequencing data reported in this paper is SRA: PRJNA597432. The raw 16S rRNA sequencing data reported in this paper is SRA: PRJNA597440.

EXPERIMENTAL MODEL AND SUBJECT DETAILS

Mosquito rearing and maintenance—*Anopheles stephensi* (strain Hor) was reared at the insectary of Fudan University at 28°C, 80% relative humidity and on a 12:12 light/dark photoperiod. *Anopheles stephensi* (strain Liston) was maintained in the Johns Hopkins Malaria Institute (JHMRI) insectary at 27°Cand 80% humidity with a 12-h day-night cycle. Adults were maintained on 2% (0.1 M) sucrose. Adult females were fed on anesthetized mice for a blood meal and were allowed to lay eggs on wet filter paper.

Plasmodium berghei maintenance—*Plasmodium berghei* ANKA parasites were maintained in BALB/c mice by serial blood passage and regular mosquito transmission (Sinden, 1997).

Plasmodium falciparum culture—*P. falciparum* NF54W was provided by the Johns Hopkins Malaria Institute (JHMRI) Core Facility. The strain was cultured as asexual stages between 0.2 and 2% parasitemia at 37°C in 4% human erythrocytes using *P. falciparum* cultures prepared as described elsewhere (Carter et al., 1993). Parasites were kept under a gas mixture of 5% O_2, 5% CO_2, and balanced N_2 for up to eight weeks according to established protocols (Trager and Jensen, 1976). Gametocytogenesis was induced by raising parasitemia > 4% and changing medium daily for 14 to 18 days to obtain matured gametocytes.

Bacteria culture—*Asaia bogorensis* strains were cultured in liquid medium (2% sorbitol, 0.5% peptone, 0.3% yeast extract, pH 3.5) or modified medium using 2% sucrose, 2% sucrose supplemented with 0.1 M glucose or 0.1 M trehalose as a carbon source at 28°C. *Enterobacter* sp. was isolated from laboratory-colonized *An. stephensi* from insectary of Fudan University and cultured in LB medium as described (Song et al., 2018).

METHOD DETAILS

Plasmodium infection of An. stephensi—Mosquitoes were blood fed on *P. berghei*-infected mice when parasitemia reached 3%–6%. Mosquitoes not fully engorged were removed 24 hr post blood meal. Fully engorged mosquitoes were maintained on 2% sucrose at 21°C until dissection. Midguts were dissected, and oocysts were counted under the microscope eight days post infection. *An. stephensi* were fed on 0.02% NF54 *P. falciparum* gametocyte cultures through artificial membranes feeders at 37°C at the Johns Hopkins Malaria Institute Core Facility as described previously (Dong et al., 2006; Trager and Jensen, 1976). Unfed mosquitoes were removed after blood feeding, and the engorged mosquitoes were kept at 27°C for eight days to check for oocysts in the midgut. To determine oocyst numbers, midguts were dissected in PBS, stained with 0.2% mercurochrome, and oocyst numbers in the midgut were counted using a phase-contrast microscope.

Metabolite extraction—Extraction of metabolites from mosquitoes was performed as described previously (Chen et al., 2018). Mosquitoes were fed on *P. berghei* infected mice with 6% parasitemia. Fifteen mosquitoes were collected and pooled for one biological sample. Ten biological replicates from each treatment were used in the following NMR analysis. Briefly, mosquitoes were snap-frozen in liquid nitrogen and homogenized in 66% methanol solution. The supernatant was saved, and pellet was re-extracted twice in the same methanol solution. All supernatants were combined and centrifuged at 16,000 g, 4°C for 10 min. Approximately 2mL of the supernatant was transferred into a new tube. Methanol was removed under a vacuum using Eppendorf Concentrator plus (Eppendorf, Germany), and the remaining liquid was lyophilized in a freeze drier.

Extraction of metabolites from liquid medium was performed as described above. Briefly, 2 mL of conditioned medium was collected from the culture with *A. bogorensis* growing for three days. Five biological replicates from each treatment were used for NMR analysis. The collected medium was mixed with 4 mL of methanol and centrifuged at 12,000 rpm, 4°C for 10 min. Approximately 2 mL of the supernatant was transferred into a new tube. Methanol

was removed under a vacuum using Eppendorf Concentrator plus (Eppendorf, Germany), and the remaining liquid was lyophilized in a freeze drier.

Each dried extract was reconstituted into 600 μL phosphate buffer (0.15 M, K_2HPO_4-NaH_2PO_4, pH 7.43) containing 80% D_2O and 0.337 mM sodium 3-trimethylsilyl [2,2,3,3-D4] propionate, TSP. After vortexing and centrifugation (16,099 g, 4°C, 10 min), 550 μL supernatant was transferred into a 5 mm NMR tube for NMR analysis.

NMR spectroscopic analysis—All NMR spectra were acquired at 298 K on a Bruker Advance III 600 MHz NMR spectrometer (600.13 MHz for proton frequency) equipped with a quaternary cryogenic inverse probe (Bruker BioSpin, Germany). ^{1}D ^{1}H NMR spectra were acquired with a standard NOESYGPPR1D pulse sequence (RD–G1–90°–t1–90°–tm–G2–90°–acq) with the recycle delay (RD) of 2 s and tm of 100 ms. The 90° pulse length was adjusted to about 10 μs, and 64 scans were collected into 32 k data points with spectral width of 20 ppm.

For NMR signal assignments purposes, a series of 2D NMR spectra were acquired for selected samples including ^{1}H–^{1}H correlation spectroscopy (COSY), ^{1}H–^{1}H total correlation spectroscopy (TOCSY), J-resolved spectroscopy (JRES), ^{1}H–^{13}C heteronuclear single quantum correlation (HSQC), and ^{1}H–^{13}C heteronuclear multiple bond correlation (HMBC) as previously reported (Dai et al., 2010a, 2010b)

Multivariate data analysis was used to analyze the metabolites from mosquito extracts one day post infection. Principal component analysis (PCA) and Orthogonal projection to latent structure discriminant analysis (OPLS-DA) were performed with the software package SIMCA-P+ (Umetrics, Sweden). PCA was conducted using the mean centered data, while OPLS-DA was carried out with 7-fold cross-validation using the unit-variance scaled data. Qualities of the OPLS-DA models were assessed via the CV-ANOVA approach with $p < 0.05$ as the significance level. The metabolites significantly changed were showed as back-transformed loadings plots from OPLS-DA with Pearson correlation coefficients color-coded for all metabolites. In these loading plots, the metabolites with warm colors (e.g., blue) contributed more significantly to the intergroup differences than those with cold colors (e.g., black).

Univariate data analysis was used to analyze the changes in metabolites in the conditioned medium from *A. bogorensis* culture. The relative content of metabolites in the extract of culture medium was calculated by the integral of characteristic and least-overlapping NMR signals. Comparisons between two groups were analyzed with Student's *t* test (if criteria were met) or nonparametric tests using MATLAB 7.1 software (Mathworks Inc., USA).

Sugar treatment—Newly-emerged *An. stephensi* were fed on the different sugar diets for up to five days. After *Plasmodium* infection, mosquitoes were maintained on 2% sucrose unless otherwise indicated. For the assay of *P. berghei* infection in mosquitoes fed with different sugar diets post blood meal, newly-emerged *An. stephensi* were fed on 2% sucrose until *Plasmodium* infection. Then, mosquitoes were maintained on different sugar meals until the oocyst number was measured. The different sugar diets were: S, 2% sucrose; G, 2%

sucrose containing D-glucose with indicated concentrations; T, 2% sucrose containing 0.1 M trehalose; 2-DG, 2% sucrose containing 0.1 M D-glucose and 5 mM 2-Deoxyo-D-glucose (2-DG); HS, 10% sucrose; $NaCHO_3$, 2% sucrose containing $NaCHO_3$ with indicated concentrations; Acetic acid, 2% sucrose + 0.1 M acetic acid; Lactic acid, 2% sucrose + 0.1 M lactic acid; Succinic acid, 2% sucrose + 0.1 M succinic acid. Sugar diets simulating the five natural plant species in West Kenya were based on the sugar composition and water content as described elsewhere (Abebe, 2015; Abere and Enoghama, 2015; Fatimah and Ahmad, 2009; Manda et al., 2007b; Sowmya et al., 2019). *R.c.*, 0.4 g D-Mannose and 0.37 g D-Gulose in 100 mL water; *S.d.*, 5.91 g D-Glucose, 0.41 g D-Fructose, 1.875 g Sucrose, 1.11 g D-Mannose, 8.31 g D-Gulose, 0.55 g D-Galactose in 100 mL water; *P.h.*, 0.06 g D-Glucose, 0.26 g D-Fructose, 0.03 g Sucrose, 0.97 g D-Gulose, 0.02 g D-Allose in 100 mL water; *T.s.*, 4.21 g D-Glucose, 11.64 g D-Fructose, 0.022 g Sucrose, 0.28 g D-Mannose, 18.96 g D-Gulose, 0.28 g D-Raffinose, 1.04 g D-Altrose in 100 mL water; *L.c.*, 0.44 g D-Glucose in 100 mL water.

Sugar measurement—Mosquitoes' hemolymph and midgut sugar levels were determined as described previously (Kwon et al., 2015; Liu et al., 2013). Briefly, 30-40 μL hemolymph from 10 mosquitoes was collected for glucose and trehalose concentration determination. Ten midguts were pooled and homogenized in 40 μL phosphate buffered saline (PBS) buffer. Thirty microliters of midgut homogenate were collected for glucose and trehalose measurement. One-third volume of individual sample was used to measure the glucose level using the Glucose Kit (Megazyme; Ireland). Another 1/3 volume was used to determine the trehalose level. The final 1/3 volume of the sample was used to extract and quantify the amount of genomic DNA (Holmes and Bonner, 1973). The concentrations of glucose and trehalose were normalized to the amount of genomic DNA. Total DNA of midguts and hemolymph was extracted using the Holmes-Bonner method (Holmes and Bonner, 1973).

Daily blood glucose level and parasitemia of *P. berghei* infected BALB/c mice were monitored from 0 to 7 dpi by collecting the blood from tail veins. Glucose level was examined with an Accu-Chek Active Blood Glucose Meter (Roche, Switzerland). Parasitemia was determined by Giemsa-stained smears of tail blood.

Antibiotics treatment—Newly-enclosed mosquitoes were administrated with fresh filtered 2% sucrose supplemented with a cocktail of antibiotics with 10 U/ml penicillin, 10 μg/mL streptomycin and 15 μg/mL gentamicin daily for up to five days (Dong et al., 2009). The efficacy of antibiotics treatment was examined by plating the homogenate of sterilized mosquitoes on LB-agars.

Oral administration of bacteria—*A. bogorensis* was isolated from the midgut of *An. stephensi* feeding on G and confirmed by 16S rRNA sequencing. Briefly, lysate from an individual midgut was cultured in liquid medium (2% sorbitol, 0.5% peptone, 0.3% yeast extract, pH 3.5) and then plated on medium containing 0.1% D-glucose, 1.5% glycerol, 0.5% peptone, 0.5% yeast extract, 0.2% malt extract, 0.7% $CaCO_3$, and 1.5% agar as described previously (Yamada et al., 2000). To re-colonize *A. bogorensis* to the antibiotic-treated *An. stephensi*, an overnight culture of this bacterium was washed twice in 0.9% NaCl

and diluted to the final concentration of 10^7–10^8 cells/ml with 2% sucrose. *A. bogorensis* containing sugar solution was introduced to antibiotics-treated mosquitoes and was changed daily. Colonization of *A. bogorensis* was examined by qRT-PCR two days post treatment. Age-matched normal and antibiotic-treated mosquitoes were used as controls. RNA was extracted from whole mosquitoes or midgut using TRIzol® (Invitrogen). One microgram of total RNA was used to synthesize cDNA using 5X All-in-One MasterMix (ABM, China). The cDNA was used as template in qPCRs with primers *A. bogorensis* 16S rRNA. The copy numbers of *A. bogorensis* and *An. stephensi S7* genes were determined using standard curves. The relative abundance of *A. bogorensis* was normalized with *An. stephensi S7* gene copy number. All primers are listed in Table S4. Quantitative real time PCR was performed using a Roche LightCycler 96 Real Time PCR Detection System using the following cycling conditions: 1 cycle of 95°C for 5 min, 40 cycles of 95°C for 15 s, 60°C for 30 s, and 72°C for 15 s. Melting curves (60°C to 95°C) were performed to confirm the identity of the PCR product. The data were processed and analyzed with LightCycler 96 software. A final concentration of ~1X10^7/mL *Enterobacter* sp. was administrated to antibiotics treated mosquitoes as described (Song et al., 2018). The homogenate of midguts one day post bacteria feeding was plated on LB agar plates.

Transcriptome analysis—Midguts of mosquitoes fed on S and G sugar meals were used for transcriptome analysis. Four mosquito midguts were pooled for one sample, and three biological replicates were collected from each treatment. Total RNA was extracted using TRIzol® Reagent according the manufacturer's instructions (Thermo Fisher, China) and sent to Majorbio (Shanghai, China) for library construction and sequencing using Illumina HiSeq xten. Clean data were aligned to the reference genome AsteS1.7 (https://vectorbase.org/organisms/anopheles-stephensi). The expression level of each transcript was calculated according to the fragments per kilobase of exon per million mapped reads (FRKM) method. R statistical package software EdgeR (Empirical analysis of Digital Gene Expression in R, http://www.bioconductor.org/packages/2.12/bioc/html/edgeR.html) was utilized for differential expression analysis.

Gene knockdown and quantitative reverse transcription PCR (qRT-PCR)—The cDNA clones of target genes were obtained using gene-specific primers (Table S4). PCR amplicons of GFP, *V-ATpase_H_N3* and *caudal* tailed with a T7 promoter (TAA TAC GAC TCA CTA TAG GGA GA) were used to synthesize dsRNAs using a MEGAscript T7 High Yield Transcription kit (Thermo Fisher, China). Four- to six-day-old females received a total 69 nL dsRNAs (4 μg/μL) through intra-thoracic microinjection using a Nanoject II microinjector (Drummond, USA). Injected mosquitoes were allowed to recover for four days prior to infection (Blandin et al., 2002). Silencing efficiency was verified by qPCR four days post dsRNA treatment using the primers listed in Table S4. The cDNA was prepared from total RNA using the 5XAll-in-One MasterMix (with AccuRT Genomic DNA Removal Kit) (ABM, China). Levels of target genes were determined by a Roche LightCycler 96 Real Time PCR Detection System with SYBR Green qPCR Master Mix (Biomake, China). The data were processed and analyzed with LightCycler 96 software. Ribosomal gene *S7* of *An. stephensi* and *18S rRNA* of *P. berghei* were used as the internal references (Baptista et al., 2010; Dimopoulos et al., 1996). Relative quantitation results were normalized with reference

genes and analyzed by the $2^{-\Delta\Delta Ct}$ method (Livak and Schmittgen, 2001). Gene expression of the dsRNA treated group was normalized to that of dsGFP controls.

Gut microbiota analysis by 16S rRNA sequencing—Mosquitoes fed on S and G sugar meals were surface sterilized with 70% ethanol twice and with 1x PBS twice. Total DNA of three midguts was pooled for one biological sample and then extracted by the method of Holmes and Bonner (Holmes and Bonner, 1973). Five biological replicates from each treatment were used for 16S rRNA analysis. The composition of microbiota of mosquitoes was analyzed using an Illumina HiSeq2500 platform in Novogene (Novogene, China) by primers targeting the V3-V4 region of bacterial *16S rRNA*. No template controls were included as controls. Following quality filtering and chimera sequences removal, a total of 772,822 reads were detected. Operational taxonomic units (OTUs) analysis was performed by Uparse software (Uparse v7.0.1001) (Edgar, 2013). Sequences with ≥ 97% similarity were assigned to the same OTUs. A total of 1,879 OTUs were obtained.

Fluorescent *in situ* hybridization—Abdomens of females fed on S and G sugar meals were fixed and sectioned as described previously (Attardo et al., 2008). Slides were hybridized with *A. bogorensis*-specific *16S rRNA* probe, Asaia1 (5′-AGC ACC AGT TTC CCG ATG TTA T-3′) and Asaia2 (5′-GAA ATA CCC ATC TCT GGA TA-3′) labeled with Alexa Fluor® 555 (Thermo Fisher, China) (Favia et al., 2007). Tissues were visualized using a Nikon ECLIPSE IVi microscope connected to a Nikon DIGITAL SIGHT DS-U3 digital camera.

Midgut pH assay—Midgut pH of *An. stephensi* was determined using m-Cresol purple (Sigma-Aldrich, China) and phenol red (Sigma-Aldrich, China). Mosquitoes were administered a sugar meal containing 2% sucrose and 0.1% m-Cresol purple or 2% sucrose and 0.04% phenol red (Overend et al., 2016; Weiss et al., 2019). The midgut was dissected six hours post feeding and visualized immediately using a ZEISS AxioCam MRc digital camera mounted on a ZEISS AXIO Zoom.V16 stereoscope.

Exflagellation assay—The midguts of mosquitoes were dissected 10 minutes after infection and kept in PCR tubes coated with heparin sodium to prevent blood clotting. After centrifugation at 2000 g for 3 min, the whole blood bolus was coated on a glass slide and stained with Giemsa. Exflagellations and exflagellation rates were calculated as described previously (Jones et al., 1994; Shinondo et al., 1994). Exflagellation events were counted per 10^5 erythrocytes under a light microscope. The exflagellation rate was calculated by the ratio of the number of exflagellation events to the number of gametocytes observed per 10^5 erythrocytes.

QUANTIFICATION AND STATISTICAL ANALYSIS

The details of statistical methods are listed in the figure legends. Data were analyzed in GraphPad Prism 8 unless otherwise indicated. The unpaired, two-tailed Student's *t* test or Mann-Whitney test were used to compare two groups depending on the normality of the data. The one-way ANOVA with different multiple comparisons tests were used to compare the difference among more than two groups depending on the normality of the data. The

statistical analysis of metabolomics data and transcriptome data are described in the corresponding methods. For correlation analysis, we divided the sugar content into groups by their medians. Then ANOVA analysis was applied to evaluate the impact of the different sugar and their combination on *A. bogorensis* load and *P. berghei* load. The ANOVA analysis was performed by using SAS proc glm (SAS Institute, USA). The number of biological replicates and the significant differences were shown in the corresponding figure legends.

Supplementary Material

Refer to Web version on PubMed Central for supplementary material.

ACKNOWLEDGMENTS

We thank Dr. Jing Yuan from Xiamen University for help with gamete staining analysis in mosquito midgut. We thank Dr. Shimin Zhao and Dr. Hongyan Wang from Fudan University for comments on manuscript. We acknowledge support from the National Institutes of Health (R01AI129819), the National Natural Science Foundation of China (U1902211 and 31822051), and the Research Fund of the State Key Laboratory of Genetic Engineering and 111 Project (B13016) from the Fudan University to J.W.

REFERENCES

Abebe S (2015). Fuel briquette potential of *Lantana camara* L. weed species and its implication for weed management and recovery of renewable energy source. In Ethiopia (Addis Ababa University).

Abere TA, and Enoghama CO (2015). Pharmacognostic standardization and insecticidal activity of the leaves of *Tecoma stans* Juss (Bignoniaceae). J. Sci. Pract. Pharm 2, 39–45.

Angrisano F, Tan YH, Sturm A, McFadden GI, and Baum J (2012). Malaria parasite colonisation of the mosquito midgut–placing the *Plasmodium* ookinete centre stage. Int. J. Parasitol 42, 519–527. [PubMed: 22406332]

Ano Y, Toyama H, Adachi O, and Matsushita K (2008). Energy metabolism of a unique acetic acid bacterium, *Asaia bogorensis*, that lacks ethanol oxidation activity. Biosci. Biotechnol. Biochem 72, 989–997. [PubMed: 18391448]

Attardo GM, Lohs C, Heddi A, Alam UH, Yildirim S, and Aksoy S (2008). Analysis of milk gland structure and function in *Glossina morsitans*: milk protein production, symbiont populations and fecundity. J. Insect Physiol 54, 1236–1242. [PubMed: 18647605]

Bahia AC, Dong Y, Blumberg BJ, Mlambo G, Tripathi A, BenMarzouk-Hidalgo OJ, Chandra R, and Dimopoulos G (2014). Exploring *Anopheles* gut bacteria for *Plasmodium* blocking activity. Environ. Microbiol 16, 2980–2994. [PubMed: 24428613]

Baptista FG, Pamplona A, Pena AC, Mota MM, Pied S, and Vigário AM (2010). Accumulation of *Plasmodium berghei*-infected red blood cells in the brain is crucial for the development of cerebral malaria in mice. Infect. Immun 78, 4033–4039. [PubMed: 20605973]

Becker A, Schlöder P, Steele JE, and Wegener G (1996). The regulation of trehalose metabolism in insects. Experientia 52, 433–439. [PubMed: 8706810]

Bennink S, Kiesow MJ, and Pradel G (2016). The development of malaria parasites in the mosquito midgut. Cell. Microbiol 18, 905–918. [PubMed: 27111866]

Billker O, Shaw MK, Margos G, and Sinden RE (1997). The roles of temperature, pH and mosquito of actors a striggers of male and female gametogenesis of *Plasmodium berghei* in vitro. Parasitology 115, 1–7. [PubMed: 9280891]

Billker O, Miller AJ, and Sinden RE (2000). Determination of mosquito bloodmeal pH in situ by ion-selective microelectrode measurement: implications for the regulation of malarial gametogenesis. Parasitology 120, 547–551. [PubMed: 10874717]

Billker O, Dechamps S, Tewari R, Wenig G, Franke-Fayard B, and Brinkmann V (2004). Calcium and a calcium-dependent protein kinase regulate gamete formation and mosquito transmission in a malaria parasite. Cell 117, 503–514. [PubMed: 15137943]

Blandin S, Moita LF, Köcher T, Wilm M, Kafatos FC, and Levashina EA (2002). Reverse genetics in the mosquito *Anopheles gambiae*: targeted disruption of the Defensin gene. EMBO Rep. 3, 852–856. [PubMed: 12189180]

Boudko DY, Moroz LL, Harvey WR, and Linser PJ (2001a). Alkalinization by chloride/bicarbonate pathway in larval mosquito midgut. Proc. Natl. Acad. Sci. USA 98, 15354–15359. [PubMed: 11742083]

Boudko DY, Moroz LL, Linser PJ, Trimarchi JR, Smith PJ, and Harvey WR (2001b). In situ analysis of pH gradients in mosquito larvae using non-invasive, self-referencing, pH-sensitive microelectrodes. J. Exp. Biol 204, 691–699. [PubMed: 11171351]

Carter R, and Nijhout MM (1977). Control of gamete formation (exflagellation) in malaria parasites. Science 195, 407–409. [PubMed: 12566]

Carter R, Ranford-Cartwright L, and Alano P (1993). The culture and preparation of gametocytes of *Plasmodium falciparum* for immunochemical, molecular, and mosquito infectivity studies. Methods Mol. Biol 21, 67–88. [PubMed: 8220736]

Chen S, Blom J, and Walker ED (2017). Genomic, physiologic, and symbiotic characterization of *Serratia marcescens* strains Isolated from the mosquito *Anopheles stephensi*. Front. Microbiol 8, 1483. [PubMed: 28861046]

Chen F, Liu C, Zhang J, Lei H, Li H-P, Liao Y-C, and Tang H (2018). Combined metabonomic and quantitative RT-PCR analyses revealed metabolic reprogramming associated with *Fusarium graminearum* resistance in transgenic *Arabidopsis thaliana*. Front. Plant Sci 8, 2177. [PubMed: 29354139]

Cirimotich CM, Dong Y, Garver LS, Sim S, and Dimopoulos G (2010). Mosquito immune defenses against *Plasmodium* infection. Dev. Comp. Immunol 34, 387–395. [PubMed: 20026176]

Cirimotich CM, Dong Y, Clayton AM, Sandiford SL, Souza-Neto JA, Mulenga M, and Dimopoulos G (2011). Natural microbe-mediated refractoriness to *Plasmodium* infection in *Anopheles gambiae*. Science 332, 855–858. [PubMed: 21566196]

Clayton AM, Cirimotich CM, Dong Y, and Dimopoulos G (2013). *Caudal* is a negative regulator of the *Anopheles* IMD pathway that controls resistance to *Plasmodium falciparum* infection. Dev. Comp. Immunol 39, 323–332. [PubMed: 23178401]

Clayton AM, Dong Y, and Dimopoulos G (2014). The *Anopheles* innate immune system in the defense against malaria infection. J. Innate Immun 6, 169–181. [PubMed: 23988482]

Corby-Harris V, Drexler A, Watkins de Jong L, Antonova Y, Pakpour N, Ziegler R, Ramberg F, Lewis EE, Brown JM, Luckhart S, and Riehle MA (2010). Activation of Akt signaling reduces the prevalence and intensity of malaria parasite infection and lifespan in *Anopheles stephensi* mosquitoes. PLoS Pathog. 6, e1001003. [PubMed: 20664791]

Dai H, Xiao C, Liu H, Hao F, and Tang H (2010a). Combined NMR and LC-DAD-MS analysis reveals comprehensive metabonomic variations for three phenotypic cultivars of *Salvia Miltiorrhiza* Bunge. J. Proteome Res 9, 1565–1578. [PubMed: 20067324]

Dai H, Xiao C, Liu H, and Tang H (2010b). Combined NMR and LC-MS analysis reveals the metabonomic changes in *Salvia miltiorrhiza* Bunge induced by water depletion. J. Proteome Res 9, 1460–1475. [PubMed: 20044832]

Deligianni E, Morgan RN, Bertuccini L, Kooij TW, Laforge A, Nahar C, Poulakakis N, Schüler H, Louis C, Matuschewski K, and Siden-Kiamos I (2011). Critical role for a stage-specific actin in male exflagellation of the malaria parasite. Cell. Microbiol 13, 1714–1730. [PubMed: 21790945]

Dimopoulos G, Richman A, della Torre A, Kafatos FC, and Louis C (1996). Identification and characterization of differentially expressed cDNAs of the vector mosquito, *Anopheles gambiae*. Proc. Natl. Acad. Sci. USA 93, 13066–13071. [PubMed: 8917545]

Domingos A, Pinheiro-Silva R, Couto J, do Rosário V, and de la Fuente J (2017). The *Anopheles gambiae* transcriptome - a turning point for malaria control. Insect Mol. Biol 26, 140–151. [PubMed: 28067439]

Dong Y, Aguilar R, Xi Z, Warr E, Mongin E, and Dimopoulos G (2006). *Anopheles gambiae* immune responses to human and rodent *Plasmodium parasite* species. PLoS Pathog. 2, e52. [PubMed: 16789837]

Dong Y, Manfredini F, and Dimopoulos G (2009). Implication of the mosquito midgut microbiota in the defense against malaria parasites. PLoS Pathog. 5, e1000423. [PubMed: 19424427]

Du S, Liu Y, Liu J, Zhao J, Champagne C, Tong L, Zhang R, Zhang F, Qin CF, Ma P, et al. (2019). *Aedes* mosquitoes acquire and transmit Zika virus by breeding in contaminated aquatic environments. Nat. Commun 10, 1324. [PubMed: 30902991]

Ebrahimi B, Jackson BT, Guseman JL, Przybylowicz CM, Stone CM, and Foster WA (2018). Alteration of plant species assemblages can decrease the transmission potential of malaria mosquitoes. J. Appl. Ecol 55, 841–851. [PubMed: 29551835]

Edgar RC (2013). UPARSE: highly accurate OTU sequences from microbial amplicon reads. Nat. Methods 10, 996–998. [PubMed: 23955772]

Fatimah H, and Ahmad T (2009). Phenology of *Parthenium hysterophorus*–a key factor for the success of its invasion. Adv. Environ. Biol 3, 150–156.

Favia G, Ricci I, Damiani C, Raddadi N, Crotti E, Marzorati M, Rizzi A, Urso R, Brusetti L, Borin S, et al. (2007). Bacteria of the genus *Asaia* stably associate with *Anopheles stephensi*, an Asian malarial mosquito vector. Proc. Natl. Acad. Sci. USA 104, 9047–9051. [PubMed: 17502606]

Foster WA (1995). Mosquito sugar feeding and reproductive energetics. Annu. Rev. Entomol 40, 443–474. [PubMed: 7810991]

Gaio Ade. O., Gusmão DS, Santos AV, Berbert-Molina MA, Pimenta PFP, and Lemos FJA (2011). Contribution of midgut bacteria to blood digestion and egg production in *aedes aegypti* (diptera: culicidae) (L.). Parasit. Vectors 4, 105. [PubMed: 21672186]

Garver LS, Dong Y, and Dimopoulos G (2009). Caspar controls resistance to *Plasmodium falciparum* in diverse anopheline species. PLoS Pathog. 5, e1000335. [PubMed: 19282971]

Gonzalez-Ceron L, Santillan F, Rodriguez MH, Mendez D, and Hernandez-Avila JE (2003). Bacteria in midguts of field-collected *Anopheles albimanus* block *Plasmodium vivax* sporogonic development. J. Med. Entomol 40, 371–374. [PubMed: 12943119]

Gouagna LC, Kerampran R, Lebon C, Brengues C, Toty C, Wilkinson DA, Boyer S, and Fontenille D (2014). Sugar-source preference, sugar intake and relative nutritional benefits in *Anopheles arabiensis* males. Acta Trop. 132, S70–S79. [PubMed: 24184355]

Gu W, Müller G, Schlein Y, Novak RJ, and Beier JC (2011). Natural plant sugar sources of *Anopheles* mosquitoes strongly impact malaria transmission potential. PLoS ONE 6, e15996. [PubMed: 21283732]

Guttery DS, Poulin B, Ramaprasad A, Wall RJ, Ferguson DJ, Brady D, Patzewitz EM, Whipple S, Straschil U, Wright MH, et al. (2014). Genome-wide functional analysis of *Plasmodium* protein phosphatases reveals key regulators of parasite development and differentiation. Cell Host Microbe 16, 128–140. [PubMed: 25011111]

Hayek SR, Rane HS, and Parra KJ (2019). Reciprocal regulation of V-ATPase and glycolytic pathway elements in health and disease. Front. Physiol 10, 127. [PubMed: 30828305]

Hien DF, Dabiré KR, Roche B, Diabaté A, Yerbanga RS, Cohuet A, Yameogo BK, Gouagna LC, Hopkins RJ, Ouedraogo GA, et al. (2016). Plant-mediated effects on mosquito capacity to transmit human malaria. PLoS Pathog. 12, e1005773. [PubMed: 27490374]

Holmes DS, and Bonner J (1973). Preparation, molecular weight, base composition, and secondary structure of giant nuclear ribonucleic acid. Biochemistry 12, 2330–2338. [PubMed: 4710584]

Itani S, Torii M, and Ishino T (2014). D-Glucose concentration is the key factor facilitating liver stage maturation of *Plasmodium*. Parasitol. Int 63, 584–590. [PubMed: 24691399]

Jacot D, Waller RF, Soldati-Favre D, MacPherson DA, and MacRae JI (2016). Apicomplexan energy metabolism: carbon source promiscuity and the quiescence hyperbole. Trends Parasitol. 32, 56–70. [PubMed: 26472327]

Jagadeshwaran U, Onken H, Hardy M, Moffett SB, and Moffett DF (2010). Cellular mechanisms of acid secretion in the posterior midgut of the larval mosquito (*Aedes aegypti*). J. Exp. Biol 213, 295–300. [PubMed: 20038664]

Jiang Y, Wei J, Cui H, Liu C, Zhi Y, Jiang Z, Li Z, Li S, Yang Z, Wang X, et al. (2020). An intracellular membrane protein GEP1 regulates xanthurenic acid induced gametogenesis of malaria parasites. Nat. Commun 11, 1764. [PubMed: 32273496]

Joët T, Eckstein-Ludwig U, Morin C, and Krishna S (2003). Validation of the hexose transporter of *Plasmodium falciparum* as a novel drug target. Proc. Natl. Acad. Sci. USA 100, 7476–7479. [PubMed: 12792024]

Jones IW, Denholm AA, Ley SV, Lovell H, Wood A, and Sinden RE (1994). Sexual development of malaria parasites is inhibited in vitro by the neem extract azadirachtin, and its semi-synthetic analogues. FEMS Microbiol. Lett 120, 267–273. [PubMed: 7980823]

Kawamoto F (1993). Ionic regulation and signal transduction system involved in the induction of gametogenesis in malaria parasites. Ann. N Y Acad. Sci 707, 431–434. [PubMed: 9137587]

Kawamoto F, Alejo-Blanco R, Fleck SL, and Sinden RE (1991). *Plasmodium berghei*: ionic regulation and the induction of gametogenesis. Exp. Parasitol 72, 33–42. [PubMed: 1993463]

Kirk K (2001). Membrane transport in the malaria-infected erythrocyte. Physiol. Rev 81, 495–537. [PubMed: 11274338]

Kwon Y, Song W, Droujinine IA, Hu Y, Asara JM, and Perrimon N (2015). Systemic organ wasting induced by localized expression of the secreted insulin/IGF antagonist ImpL2. Dev. Cell 33, 36–46. [PubMed: 25850671]

Lanfrancotti A, Bertuccini L, Silvestrini F, and Alano P (2007). *Plasmodium falciparum*: mRNA co-expression and protein co-localisation of two gene products upregulated in early gametocytes. Exp. Parasitol 116, 497–503. [PubMed: 17367781]

LeRoux M, Lakshmanan V, and Daily JP (2009). *Plasmodium falciparum* biology: analysis of in vitro versus in vivo growth conditions. Trends Parasitol. 25, 474–481. [PubMed: 19747879]

Li JV, Wang Y, Saric J, Nicholson JK, Dirnhofer S, Singer BH, Tanner M, Wittlin S, Holmes E, and Utzinger J (2008). Global metabolic responses of NMRI mice to an experimental *Plasmodium berghei* infection. J. Proteome Res 7, 3948–3956. [PubMed: 18646786]

Linser PJ, Smith KE, Seron TJ, and Neira Oviedo M (2009). Carbonic anhydrases and anion transport in mosquito midgut pH regulation. J. Exp. Biol 212, 1662–1671. [PubMed: 19448076]

Liu K, Dong Y, Huang Y, Rasgon JL, and Agre P (2013). Impact of trehalose transporter knockdown on *Anopheles gambiae* stress adaptation and susceptibility to *Plasmodium falciparum* infection. Proc. Natl. Acad. Sci. USA 110, 17504–17509. [PubMed: 24101462]

Livak KJ, and Schmittgen TD (2001). Analysis of relative gene expression data using real-time quantitative PCR and the $2(^{-\Delta\Delta C(T)})$ Method. Methods 25, 402–408. [PubMed: 11846609]

Luckhart S, Giulivi C, Drexler AL, Antonova-Koch Y, Sakaguchi D, Napoli E, Wong S, Price MS, Eigenheer R, Phinney BS, et al. (2013). Sustained activation of Akt elicits mitochondrial dysfunction to block *Plasmodium falciparum* infection in the mosquito host. PLoS Pathog. 9, e1003180. [PubMed: 23468624]

Mancio-Silva L, Slavic K, Grilo Ruivo MT, Grosso AR, Modrzynska KK, Vera IM, Sales-Dias J, Gomes AR, MacPherson CR, Crozet P, et al. (2017). Nutrient sensing modulates malaria parasite virulence. Nature 547, 213–216. [PubMed: 28678779]

Manda H, Gouagna L-C, Nyandat E, Kabiru EW, Jackson RR, Foster WA, Githure JI, Beier JC, and Hassanali A (2007a). Discriminative feeding behaviour of *Anopheles gambiae* s.s. on endemic plants in western Kenya. Med. Vet. Entomol 21, 103–111. [PubMed: 17373953]

Manda H, Gouagna LC, Foster WA, Jackson RR, Beier JC, Githure JI, and Hassanali A (2007b). Effect of discriminative plant-sugar feeding on the survival and fecundity of *Anopheles gambiae*. Malar. J 6, 113. [PubMed: 17711580]

Marques SR, Ramakrishnan C, Carzaniga R, Blagborough AM, Delves MJ, Talman AM, and Sinden RE (2015). An essential role of the basal body protein SAS-6 in *Plasmodium* male gamete development and malaria transmission. Cell. Microbiol 17, 191–206. [PubMed: 25154861]

McKee RW, Ormsbee RA, Anfinsen CB, Geiman QM, and Ball EG (1946). Studies on malarial parasites: VI. The chemistry and metabolism of normal and parasitized (*P. knowlesi*) monkey blood. J. Exp. Med 84, 569–582. [PubMed: 19871589]

Meireles P, Sales-Dias J, Andrade CM, Mello-Vieira J, Mancio-Silva L, Simas JP, Staines HM, and Prudêncio M (2017). GLUT1-mediated glucose uptake plays a crucial role during *Plasmodium* hepatic infection. Cell. Microbiol 19, e12646.

Minard G, Tran FH, Raharimalala FN, Hellard E, Ravelonandro P, Mavingui P, and Valiente Moro C (2013). Prevalence, genomic and metabolic profiles of *Acinetobacter* and *Asaia* associated with field-caught *Aedes albopictus* from Madagascar. FEMS Microbiol. Ecol 83, 63–73. [PubMed: 22808994]

Olivieri A, Bertuccini L, Deligianni E, Franke-Fayard B, Currà C, Siden-Kiamos I, Hanssen E, Grasso F, Superti F, Pace T, et al. (2015). Distinct properties of the egress-related osmiophilic bodies in male and female gametocytes of the rodent malaria parasite *Plasmodium berghei*. Cell. Microbiol 17, 355–368. [PubMed: 25262869]

Olszewski KL, and Llinás M (2011). Central carbon metabolism of *Plasmodium* parasites. Mol. Biochem. Parasitol 175, 95–103. [PubMed: 20849882]

Overend G, Luo Y, Henderson L, Douglas AE, Davies SA, and Dow JA (2016). Molecular mechanism and functional significance of acid generation in the *Drosophila* midgut. Sci. Rep 6, 27242. [PubMed: 27250760]

Pakpour N, Corby-Harris V, Green GP, Smithers HM, Cheung KW, Riehle MA, and Luckhart S (2012). Ingested human insulin inhibits the mosquito NF-κB-dependent immune response to *Plasmodium falciparum*. Infect. Immun 80, 2141–2149. [PubMed: 22473605]

Patrick ML, Aimanova K, Sanders HR, and Gill SS (2006). P-type Na+/K+-ATPase and V-type H+-ATPase expression patterns in the osmoregulatory organs of larval and adult mosquito *Aedes aegypti*. J. Exp. Biol 209, 4638–4651. [PubMed: 17114398]

Pietri JE, Pietri EJ, Potts R, Riehle MA, and Luckhart S (2015). *Plasmodium falciparum* suppresses the host immune response by inducing the synthesis of insulin-like peptides (ILPs) in the mosquito *Anopheles stephensi*. Dev. Comp. Immunol 53, 134–144. [PubMed: 26165161]

Pietri JE, Pakpour N, Napoli E, Song G, Pietri E, Potts R, Cheung KW, Walker G, Riehle MA, Starcevich H, et al. (2016). Two insulin-like peptides differentially regulate malaria parasite infection in the mosquito through effects on intermediary metabolism. Biochem. J 473, 3487–3503. [PubMed: 27496548]

Ponzi M, Sidén-Kiamos I, Bertuccini L, Currà C, Kroeze H, Camarda G, Pace T, Franke-Fayard B, Laurentino EC, Louis C, et al. (2009). Egress of *Plasmodium berghei* gametes from their host erythrocyte is mediated by the MDV-1/PEG3 protein. Cell. Microbiol 11, 1272–1288. [PubMed: 19438517]

Pumpuni CB, Demaio J, Kent M, Davis JR, and Beier JC (1996). Bacterial population dynamics in three anopheline species: the impact on *Plasmodium* sporogonic development. Am. J. Trop. Med. Hyg 54, 214–218. [PubMed: 8619451]

Ricci I, Damiani C, Capone A, DeFreece C, Rossi P, and Favia G (2012). Mosquito/microbiota interactions: from complex relationships to biotechnological perspectives. Curr. Opin. Microbiol 15, 278–284. [PubMed: 22465193]

Roth EF Jr. (1987). Malarial parasite hexokinase and hexokinase-dependent glutathione reduction in the *Plasmodium falciparum*-infected human erythrocyte. J. Biol. Chem 262, 15678–15682. [PubMed: 3316204]

Saliba KJ, Krishna S, and Kirk K (2004). Inhibition of hexose transport and abrogation of pH homeostasis in the intraerythrocytic malaria parasite by an O-3-hexose derivative. FEBS Lett. 570, 93–96. [PubMed: 15251446]

Samaddar N, Paul A, Chakravorty S, Chakraborty W, Mukherjee J, Chowdhuri D, and Gachhui R (2011). Nitrogen fixation in *Asaia* sp. (family Acetobacteraceae). Curr. Microbiol 63, 226–231. [PubMed: 21681635]

Sebastian S, Brochet M, Collins MO, Schwach F, Jones ML, Goulding D, Rayner JC, Choudhary JS, and Billker O (2012). A *Plasmodium* calcium-dependent protein kinase controls zygote development and transmission by translationally activating repressed mRNAs. Cell Host Microbe 12, 9–19. [PubMed: 22817984]

Shinondo CJ, Lanners HN, Lowrie RC Jr., and Wiser MF (1994). Effect of pyrimethamine resistance on sporogony in a *Plasmodium berghei/Anopheles stephensi* model. Exp. Parasitol 78, 194–202. [PubMed: 8119374]

Sinden RE (1997). Infection of mosquitoes with rodent malaria. In The molecular biology of insect disease vectors, Crampton JM, Beard CB, and Louis C, eds. (Springer), pp. 67–91.

Slavic K, Delves MJ, Prudêncio M, Talman AM, Straschil U, Derby-shire ET, Xu Z, Sinden RE, Mota MM, Morin C, et al. (2011). Use of a selective inhibitor to define the chemotherapeutic potential of the plasmodial hexose transporter in different stages of the parasite's life cycle. Antimicrob. Agents Chemother 55, 2824–2830. [PubMed: 21402842]

Smith RC, Vega-Rodríguez J, and Jacobs-Lorena M (2014). The *Plasmodium* bottleneck: malaria parasite losses in the mosquito vector. Mem. Inst. Oswaldo Cruz 109, 644–661. [PubMed: 25185005]

Song X, Wang M, Dong L, Zhu H, and Wang J (2018). PGRP-LD mediates *A. stephensi* vector competency by regulating homeostasis of micro-biota-induced peritrophic matrix synthesis. PLoS Pathog. 14, e1006899. [PubMed: 29489896]

Sowmya P, Vanaja M, Sunita V, and Raghuram Reddy P (2019). Genetic advance for physiological parameters in two high yielding castor (*Ricinus communis* L.) genotypes under irrigation and moisture stress. J. Pharmacogn. Phytochem SP2, 179–184.

Stone CM, Jackson BT, and Foster WA (2012). Effects of plant-community composition on the vectorial capacity and fitness of the malaria mosquito *Anopheles gambiae*. Am. J. Trop. Med. Hyg 87, 727–736. [PubMed: 22927493]

Sturm A, Mollard V, Cozijnsen A, Goodman CD, and McFadden GI (2015). Mitochondrial ATP synthase is dispensable in blood-stage *Plasmodium berghei* rodent malaria but essential in the mosquito phase. Proc. Natl. Acad. Sci. USA 112, 10216–10223. [PubMed: 25831536]

Talman AM, Lacroix C, Marques SR, Blagborough AM, Carzaniga R, Ménard R, and Sinden RE (2011). PbGEST mediates malaria transmission to both mosquito and vertebrate host. Mol. Microbiol 82, 462–474. [PubMed: 21958024]

Theriot CM, Koenigsknecht MJ, Carlson PE Jr., Hatton GE, Nelson AM, Li B, Huffnagle GB, Z Li J, and Young VB (2014). Antibiotic-induced shifts in the mouse gut microbiome and metabolome increase susceptibility to *Clostridium difficile* infection. Nat. Commun 5, 3114. [PubMed: 24445449]

Trager W, and Jensen JB (1976). Human malaria parasites in continuous culture. Science 193, 673–675. [PubMed: 781840]

Wang S, Ghosh AK, Bongio N, Stebbings KA, Lampe DJ, and Jacobs-Lorena M (2012). Fighting malaria with engineered symbiotic bacteria from vector mosquitoes. Proc. Natl. Acad. Sci. USA 109, 12734–12739. [PubMed: 22802646]

Weiss BL, Maltz MA, Vigneron A, Wu Y, Walter KS, O'Neill MB, Wang J, and Aksoy S (2019). Colonization of the tsetse fly midgut with commensal *Kosakonia cowanii* Zambiae inhibits trypanosome infection establishment. PLoS Pathog. 15, e1007470. [PubMed: 30817773]

Yamada Y, Katsura K, Kawasaki H, Widyastuti Y, Saono S, Seki T, Uchimura T, and Komagata K (2000). *Asaia bogorensis* gen. nov., sp. nov., an unusual acetic acid bacterium in the alpha-*Proteobacteria*. Int. J. Syst. Evol. Microbiol 50, 823–829. [PubMed: 10758893]

Yeoh LM, Goodman CD, Mollard V, McFadden GI, and Ralph SA (2017). Comparative transcriptomics of female and male gametocytes in *Plasmodium berghei* and the evolution of sex in alveolates. BMC Genomics 18, 734. [PubMed: 28923023]

Yoshimori T, Yamamoto A, Moriyama Y, Futai M, and Tashiro Y (1991). Bafilomycin A1, a specific inhibitor of vacuolar-type H(+)-ATPase, inhibits acidification and protein degradation in lysosomes of cultured cells. J. Biol. Chem 266, 17707–17712. [PubMed: 1832676]

Yu BT, Ding YM, Mo XC, Liu N, Li HJ, and Mo JC (2016). Survivor-ship and fecundity of *Culex pipiens* pallens feeding on flowering plants and seed pods with differential preferences. Acta Trop. 155, 51–57. [PubMed: 26739652]

Yuda M, Iwanaga S, Kaneko I, and Kato T (2015). Global transcriptional repression: An initial and essential step for *Plasmodium* sexual development. Proc. Natl. Acad. Sci. USA 112, 12824–12829. [PubMed: 26417110]

Yuval B, Holliday-Hanson ML, and Washing RK (1994). Energy budget of swarming male mosquitoes. Ecol. Entomol 19, 74–78.

Zhuang Z, Linser PJ, and Harvey WR (1999). Antibody to H(+) V-ATPase subunit E colocalizes with portasomes in alkaline larval midgut of a freshwater mosquito (*Aedes aegypti*). J. Exp. Biol 202, 2449–2460. [PubMed: 10460732]

Zielke HR, Zielke CL, and Ozand PT (1984). Glutamine: a major energy source for cultured mammalian cells. Fed. Proc 43, 121–125. [PubMed: 6690331]

Highlights

- Glucose/trehalose supplementation promotes *Plasmodium* infection in mosquitoes
- Glucose/trehalose supplementation promotes the expansion of a gut commensal *Asaia*
- *Asaia* remodels glucose metabolism and increases midgut pH
- The pH increase induces *Plasmodium* gametogenesis and facilitates parasite infection

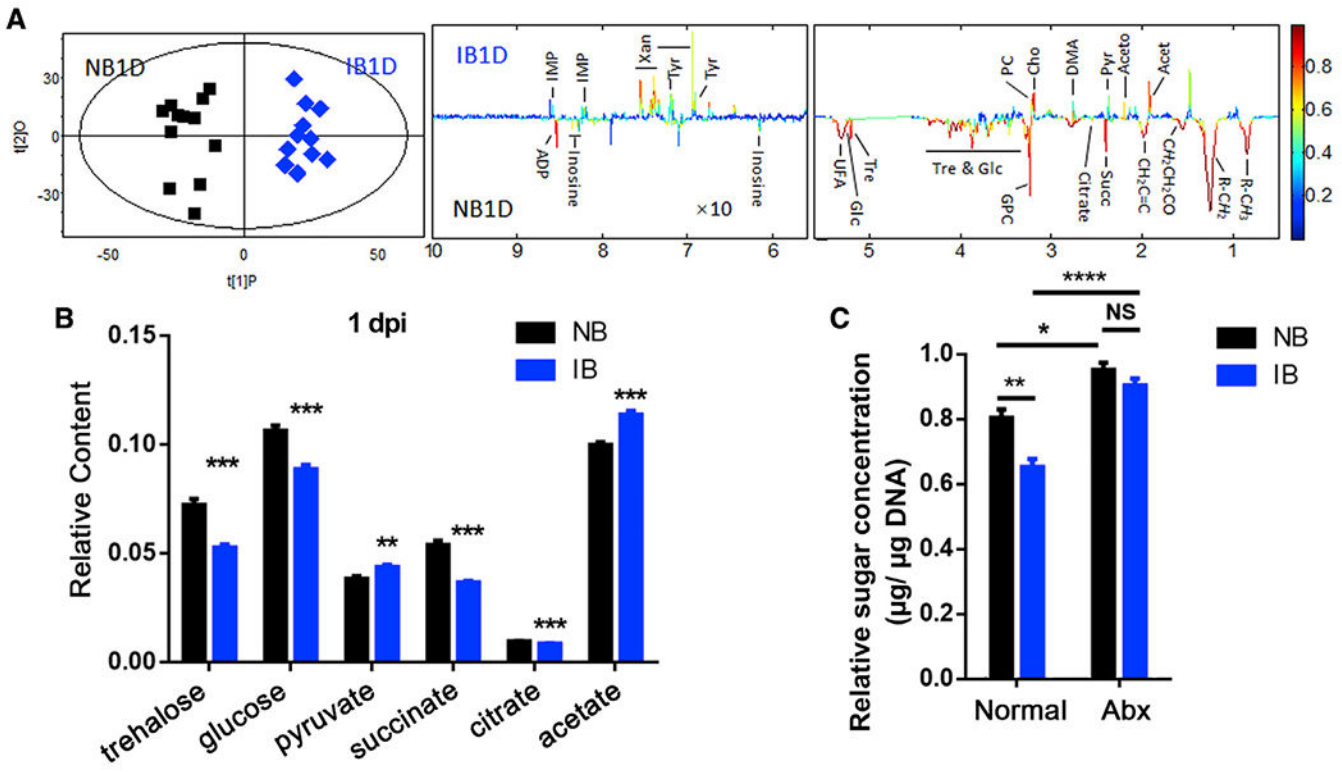

Figure 1. ***P. berghei*** **infection changes glucose metabolism in** ***An. Stephensi***

(A) OPLS-DA score plots (left) and corresponding loading plots (right) show the metabolites significantly changed in the extract from mosquitoes fed on normal blood (NB) and infectious blood (IB) at 1 day post-infection (1 dpi). R2X = 0.430, Q2 = 0.857. Metabolite keys are the same as in Table S1.

(B) Relative content of the key sugar metabolites. All of the integral regions were normalized to dried weight of mosquitoes for each spectrum.

(C) The relative concentrations of total sugar levels (glucose and trehalose) in the midgut of mosquitoes treated without (Normal) or with antibiotics (Abx) 1 dpi. Glucose and trehalose concentrations were normalized to genomic DNA extracted from the midgut.

Significance in (A) was determined by a cross-validated ANOVA (CV-ANOVA) approach with $p < 0.05$ as the significance level. Significance in (B) was determined by Student's t test. Significance in (C) was determined by ANOVA with Tukey test. Error bars indicate SEM (n = 5). NS, not significant, *$p < 0.05$, **$p < 0.01$, ***$p < 0.001$, ****$p < 0.0001$. See also Figure S1.

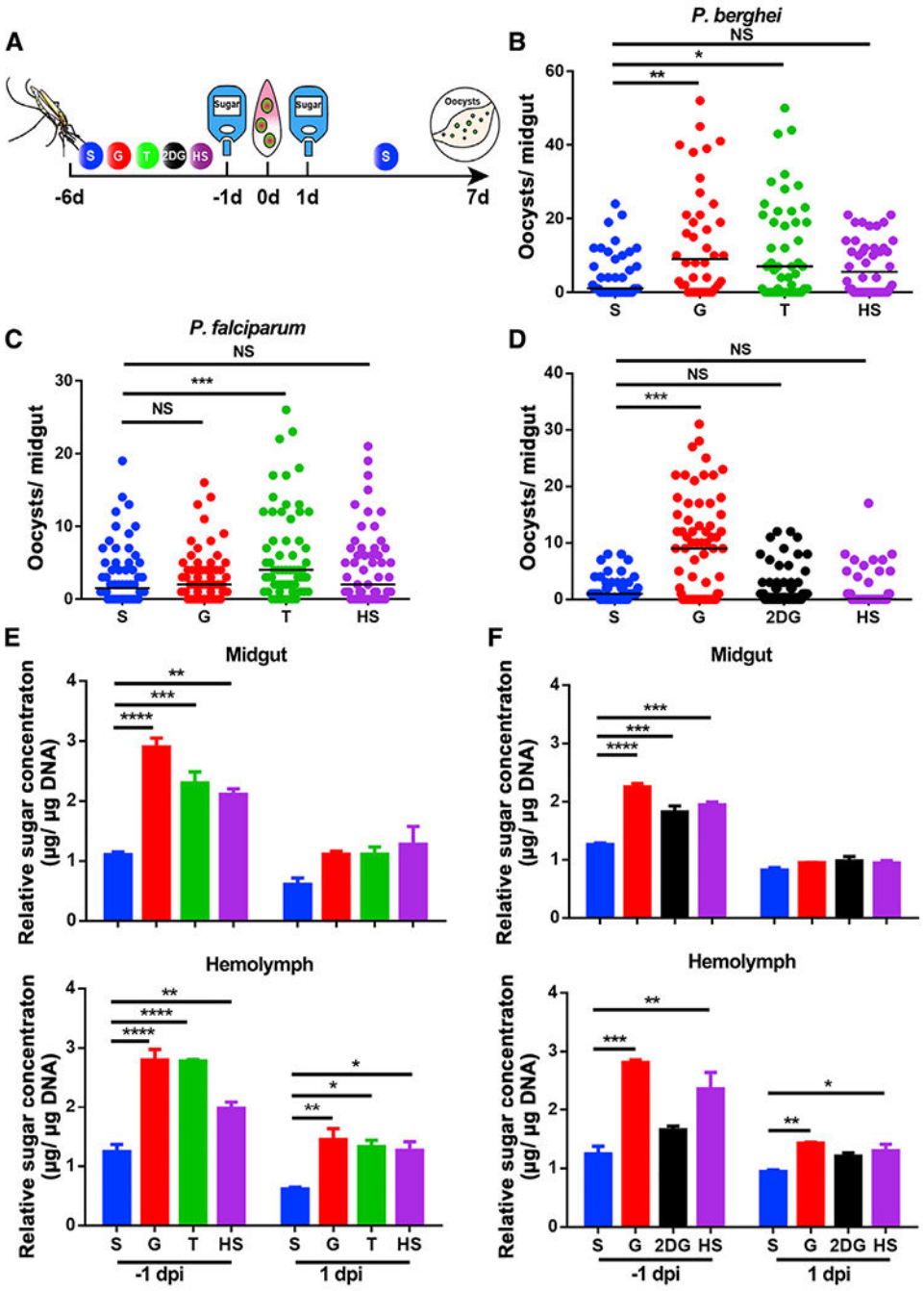

Figure 2. Glucose and trehalose supplementation promote *Plasmodium* infection in *An. Stephensi*

(A) Workflow of sugar treatment on *Anopheles* mosquitoes.

(B and C) *P. berghei* and *P. falciparum* oocyst intensities in mosquitoes fed with S, G, T, and HS diets.

(D) *P. berghei* oocyst intensity in mosquitoes fed with S, G, 2-DG, and HS diets.

(E and F) The relative concentration of total sugar (glucose and trehalose) in the midgut (top) and hemolymph (bottom) of mosquitoes fed on the sugar diets corresponding to (B) and (D), respectively, one day prior to infection (−1 dpi) and 1 dpi. Glucose and trehalose

concentrations were normalized to the amounts of genomic DNA extracted from midgut and hemolymph, respectively.

Each dot represents an individual mosquito, and horizontal lines represent the medians. Results shown in (B)–(D) were pooled from at least two independent experiments. Significance was determined by ANOVA with Dunn's tests. Significance in (E) and (F) was determined by ANOVA with Dunnett tests. Error bars indicate SEM (n = 5). *p < 0.05, **p < 0.01, ***p < 0.001, ****p < 0.0001. S, 2% sucrose; G, 2% sucrose + 0.1 M glucose; T, 2% sucose + 0.1 M trehalose; 2-DG, 2% sucrose + 0.1 M glucose + 5 mM 2-DG; HS, 10% sucrose. See also Figure S2.

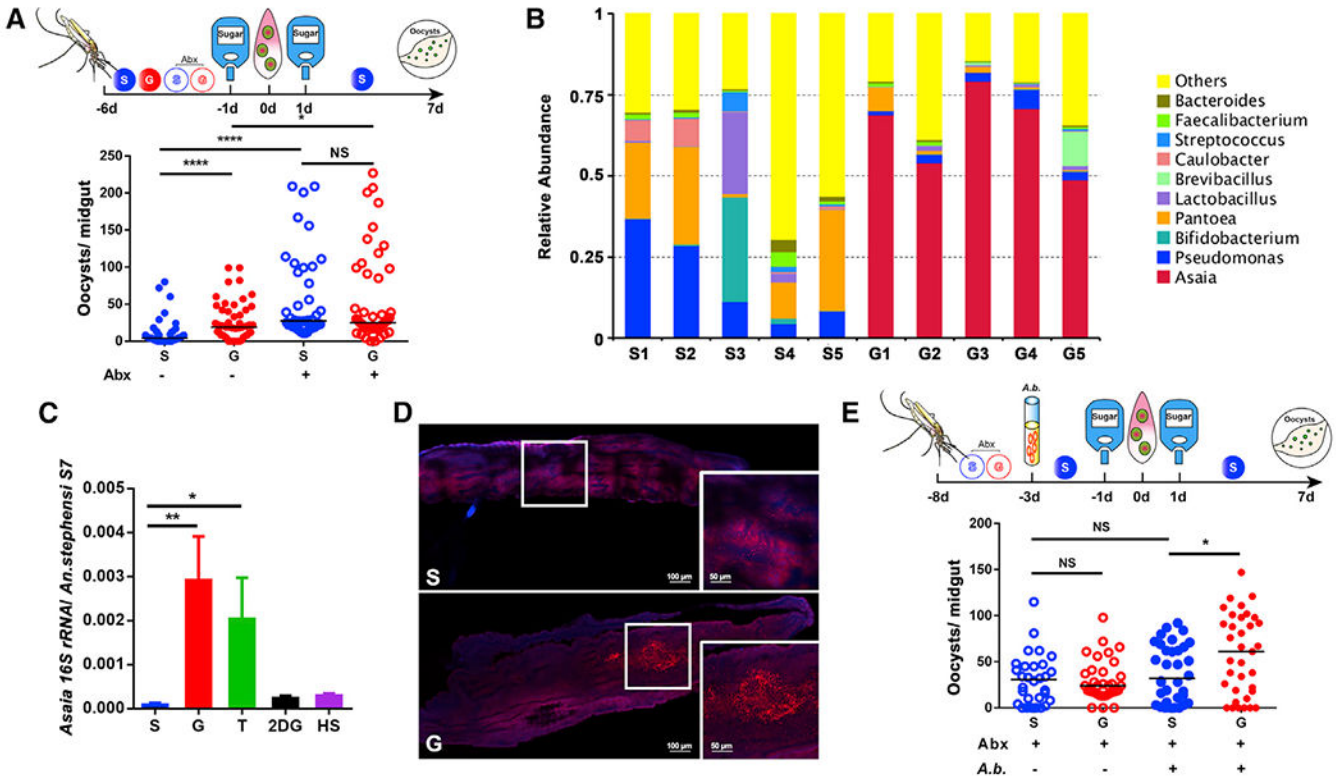

Figure 3. *Asaia bogorensis* promotes *P. berghei* infection in *An. stephensi*

(A) Influence of antibiotics treatment on *P. berghei* infection.

(B) Relative abundance of major bacteria genera in the midguts of *An. stephensi* fed on S and G by 16S rRNA pyrosequencing. Each column represents three pooled midguts.

(C) The abundance of *A. bogorensis* in the midgut of *An. stephensi* determined by qPCR.

(D) Localization of *A. bogorensis* (red) in the midgut of *An. stephensi* fed on S and G, using *A. bogorensis*-specific probes. Nuclei were stained with DAPI (blue). The enlarged view in the box is shown on the right of the figure. Images are representative of at least five individual mosquito midguts.

(E) Influence of *A. bogorensis* re-colonization on *P. berghei* infection outcome.

Each dot represents an individual mosquito, and horizontal lines represent the medians. Results shown in (A) and (E) were pooled from two independent experiments. Significance was determined by ANOVA with Dunn's tests. Significance in (C) was determined by ANOVA with Dunnett tests. Error bars indicate SEM (n = 12). NS, not significant, *p < 0.05, **p < 0.01, ****p < 0.0001. S, 2% sucrose; G, 2% sucrose + 0.1 M glucose; Abx, antibiotics treatment; *A.b., A. bogorensis*. See also Figure S3.

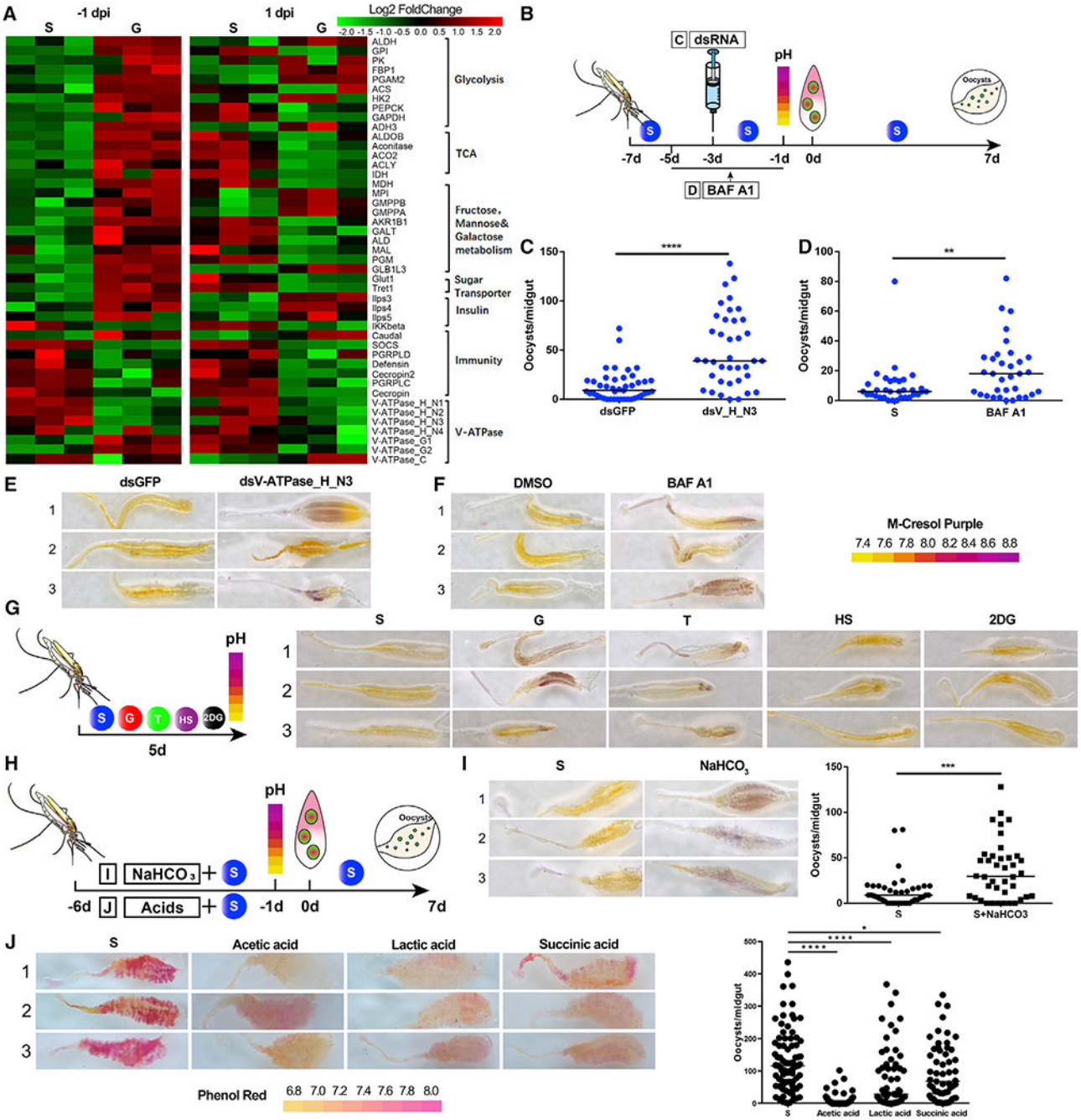

Figure 4. Midgut pH determines the susceptibility of *An. stephensi* to *P. berghei* infection

(A) Hierarchical clustering analysis of differentially expressed genes in the midguts of mosquitoes fed with S and G at −1 dpi and 1 dpi. Upregulated genes are shown in red; downregulated genes are shown in green.

(B) Workflow of dsRNA injection (C) and BAF A1 treatment (D) in *An. stephensi*.

(C and D) *P. berghei* oocyst numbers in dsRNA (C) and BAF A1 (D) treatments.

(E and F) The pH staining of mosquito midguts treated with dsRNA (E) and BAF A1 (F) by pH indicator m-cresol purple. The pH indicator is shown on the right. Images are three representatives of at least five individual mosquito midguts.

(G) The pH staining of mosquito midguts fed on S, G, T, HS, and 2-DG diets by m-cresol purple. Workflow of pH assay of mosquitoes on S, G, T, HS, and 2-DG diets (left). The pH staining of midguts on different diets (right). Images are three representatives of at least five individual mosquito midguts.

(H) Workflow of $NaCHO_3$ (I) and acids treatments (J) in *An. stephensi*.

(I) The effect of $NaCHO_3$ supplementation on *P. berghei* infection. The pH staining of $NaHCO_3$-fed midguts (left) and *Plasmodium* oocyst numbers after $NaHCO_3$ treatment (right). Images are three representatives of at least five individual mosquito midguts.

(J) The effect of acid supplementation on *P. berghei* infection. The pH staining of midguts on different diets is shown by pH indicator phenol red (left). The pH indicator is shown at the bottom. The *Plasmodium* oocyst numbers after acid treatment are shown (right). Images are three representatives of at least five individual mosquito midguts.

Each dot represents an individual mosquito, and horizontal lines represent the medians. Data shown in (C), (D), (I), and (J) were pooled from two independent experiments. Significance was determined by Mann-Whitney test in (C), (D), and (I) and by ANOVA with Dunn's tests in (J). *$p < 0.05$, **$p < 0.01$, ***$p < 0.001$, ****$p < 0.0001$. S, 2% sucrose; G, 2% sucrose + 0.1 M glucose; T, 2% sucrose + 0.1 M trehalose; 2-DG, 2% sucrose + 0.1 M glucose + 5 mM 2-DG; HS, 10% sucrose, $NaCHO_3$, 2% sucrose + 0.1 M $NaCHO_3$. See also Table S2 and Figure S4.

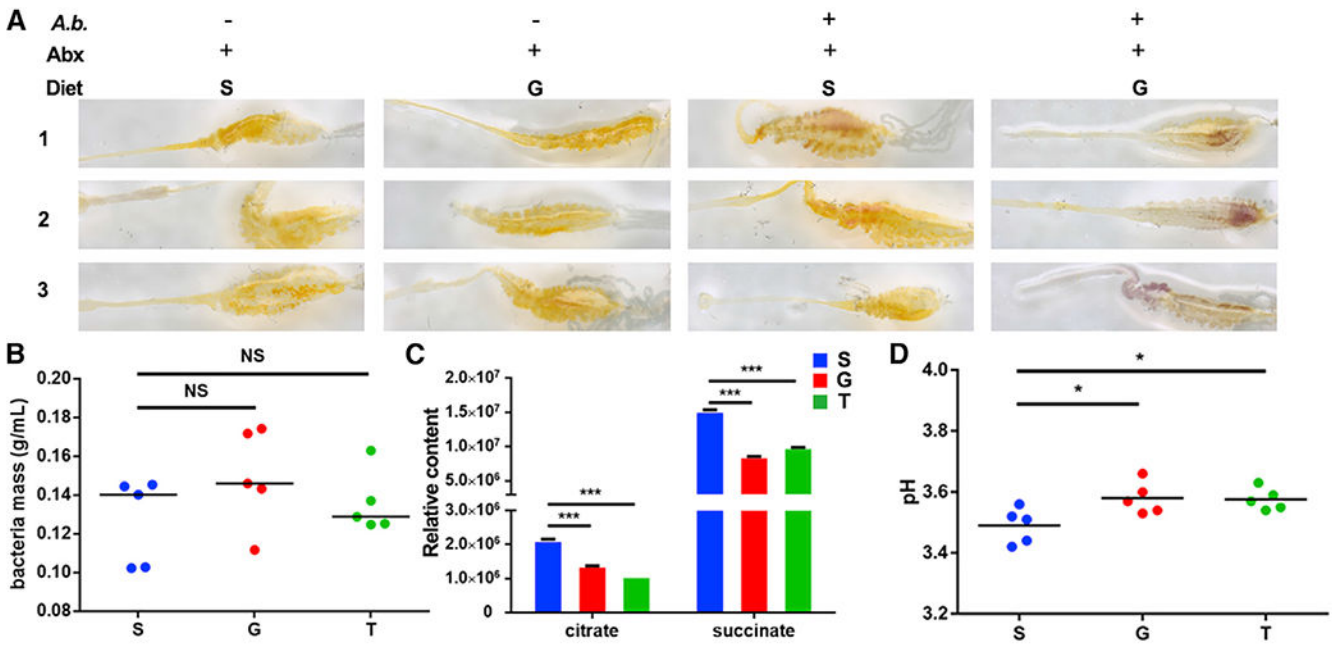

Figure 5. Glucose metabolic activity of *A. bogorensis* determines the midgut pH

(A) Influence of *A. bogorensis* re-colonization on the pH of the mosquito midgut. Images are three representatives of at least five individual mosquito midguts.

(B) Bacterial mass of *A. bogorensis* grown in S, G, and T.

(C) Relative content of the key sugar metabolites in the three conditioned media.

(D) The pH value of S (blue), G (red), and T (green) containing media 3 days post-*A. bogorensis* growth.

Significance in (B)–(D) was determined by ANOVA with Dunnett tests. Errorbars indicate SEM (n = 5). NS, not significant, *p < 0.05, ***p < 0.001. S, 2% sucrose; G, 2% sucrose + 0.1 M glucose; T, 2% sucrose + 0.1 M trehalose. See also Figure S4.

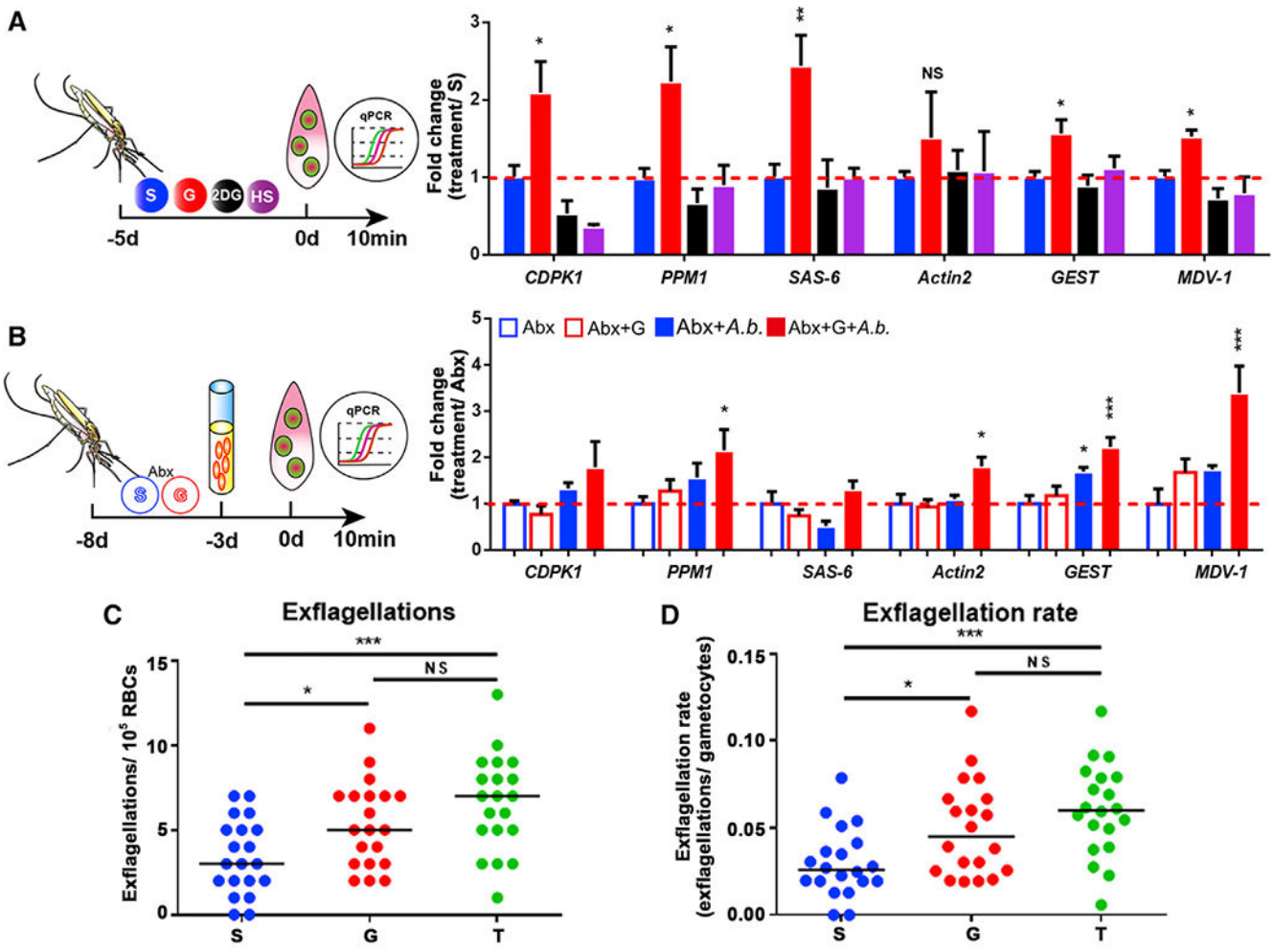

Figure 6. The increase of pH induces male gametogenesis

(A) Quantification of the mRNA abundance of genes associated with male gametogenesis in mosquitoes fed with S, G, 2-DG, and HS.

(B) Quantification of the mRNA abundance of genes associated with male gametogenesis in *A. bogorensis* re-colonized mosquitoes fed with S and G.

(C and D) Exflagellations and exflagellation rate in the mosquitoes fed on S, G, and T. Exflagellations were monitored 10 min post-infection. The median number of exflagellations per 10^5 erythrocytes is shown (C), and exflagellation rate was shown as the percent (exflagellations/gametocytes) per 10^5 erythrocytes (D).

Significance in (A) and (B) was determined by ANOVA followed by Dunnett's tests. Error bars indicate SEM (n = 5). Each dot represents one mosquito, and horizontal lines represent the medians in (C) and (D). Data shown in (C) and (D) were pooled from two independent experiments. Significance was determined by ANOVA followed by Holm Sidak's tests. NS, not significant, *p < 0.05, **p < 0.01, ***p < 0.001. S, 2% sucrose; G, 2% sucrose + 0.1 M glucose; T, 2% sucrose + 0.1 M trehalose; 2-DG, 2% sucrose + 0.1 M glucose + 5 mM 2-DG; HS, 10% sucrose. See also Figure S5.

A

Content (g/mL)	S	G	*P.h.*	*L.c.*	*R.c.*	*T.s.*	*S.d.*
sucrose	0.02	0.02	0.03	NA	NA	0.022	1.875
D-Glucose	NA	0.02	0.06	0.44	NA	4.21	5.91
D-Mannose	NA	NA	NA	NA	0.4	0.28	1.11
D-Gulose	NA	NA	0.97	NA	0.37	18.96	8.31
D-Fructose	NA	NA	0.26	NA	NA	11.64	0.41
D-Galactose	NA	NA	NA	NA	NA	NA	0.55
D-Allose	NA	NA	0.02	NA	NA	NA	NA
D-Raffinose	NA	NA	NA	NA	NA	0.28	NA
D-Altrose	NA	NA	NA	NA	NA	1.04	NA

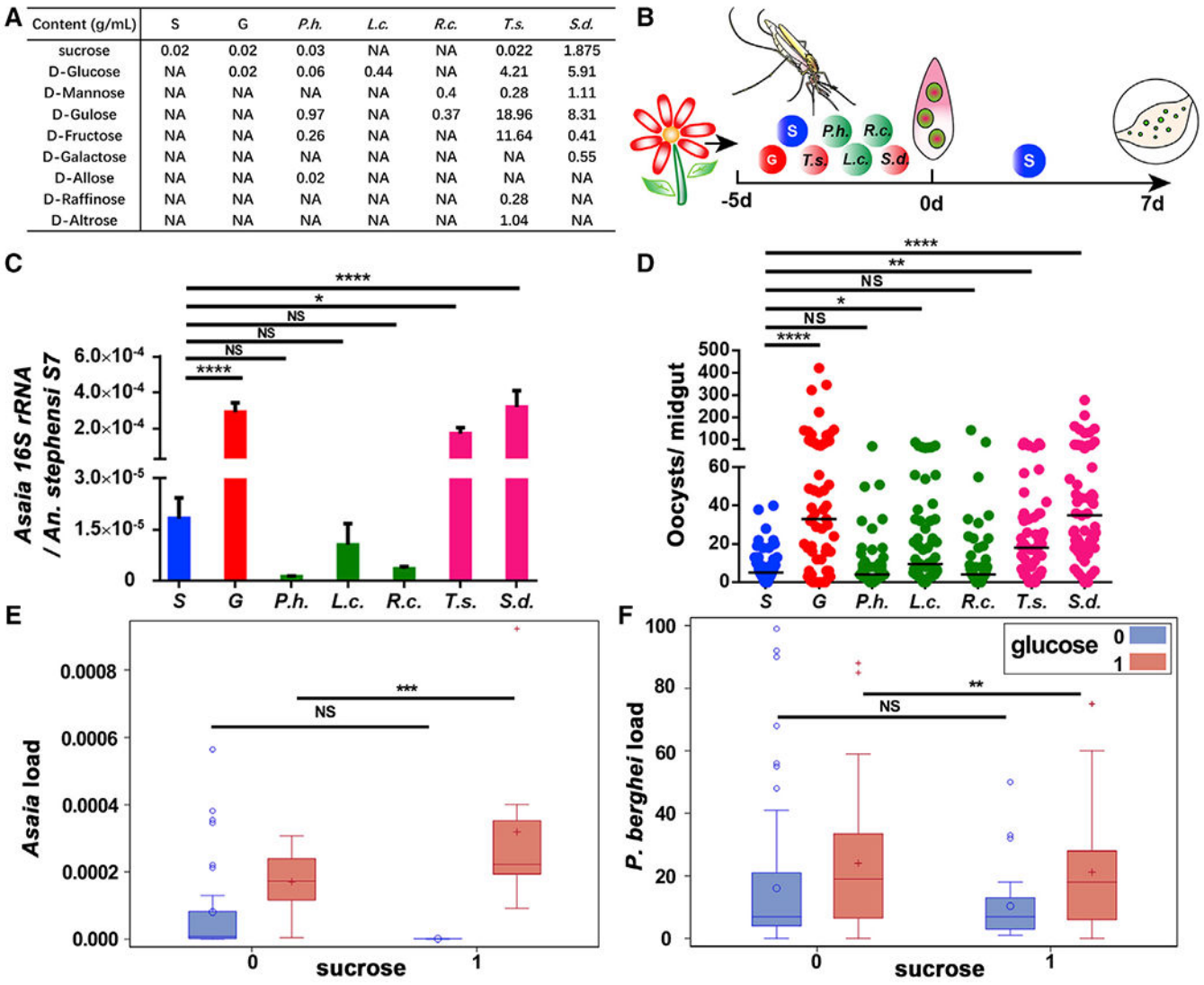

Figure 7. Sugar composition affects the abundance of *A. bogorensis* and *P. berghei* infection outcome

(A) Recipe for sugar solution simulating natural plant nectar.

(B) Workflow of sugar treatments in *An. stephensi*.

(C) Quantification of levels of *A. bogorensis* in mosquitoes fed on different sugar diets.

(D) Oocyst number in mosquitoes fed on different sugar diets.

(E and F) Boxplots of *A. bogorensis* load (E) and oocyst number (F) in each sugar composition group (sucrose = 0 indicates sucrose content no more than 0.022 g/mL in this group; sucrose = 1 indicates sucrose content higher than 0.022 g/mL in this group; glucose = 0 indicates content no more than 0.44 g/mL; glucose = 1 indicates content higher than 0.44 g/mL).

Significance in (C) was determined by ANOVA followed by Dunnett's test. Error bars indicate SEM (n = 12). Each dot represents an individual mosquito, and horizontal lines represent the medians in (D). Data shown in (D) were pooled from two independent experiments. Significance in (D) was determined by ANOVA with Dunn's tests.

Significance in (E) and (F) was estimated by using variance analysis. Sucrose and glucose contents in (E) and (F) were both divided into categorical variables by their medians (0.022 g/mL and 0.44 g/mL, respectively). NS = not significant, *p < 0.05, **p < 0.01, ***p < 0.001, ****p < 0.0001. S, 2% sucrose; G, 2% sucrose + 0.1 M glucose; *P.h., P. hysterophorus; R.c., R. communis; L.c., L. camara; T.s., T. stans; S.d., S. didymobotrya*.

KEY RESOURCES TABLE

REAGENT or RESOURCE	SOURCE	IDENTIFIER
Bacterial and virus strains		
Asaia bogorensis	This paper	N/A
Enterobacter sp.	This paper	N/A
Chemicals, peptides, and recombinant proteins		
D-glucose	Sangon	Cat#10010518
D-trehalose	Biotech	Cat#A500966
2-Deoxyo-D-glucose	Sigma-Aldrich	Cat#D8375
Sucrose	Sangon	Cat#10021418
D-fructose 1,6-bisphosphate trisodium salt	Santa cruz	Cat#214805A
D-glucose-6-phosphate monosodium salt	Santa cruz	Cat#210728A
Sodium pyruvate	Sangon	Cat#A600884
D-raffinose	Aladdin	Cat#R111688
D-mannose	Aladdin	Cat#M103969
D-allose	Sangon	Cat#A606673
D-galactose	aladdin	Cat#G100369
D-altrose	aladdin	Cat#A111909
D-gulose	aladdin	Cat#G120861
Penicillin-streptomycin	Thermo Fisher	Cat#15070063
Gentamicin	Sigma-Aldrich	Cat#G1914
M-cresol purple	Sigma-Aldrich	Cat#857890
Succinic acid	Sangon	Cat#A610496
Lactic acid	Sangon	Cat#A50404
Acetic acid	SCR	Cat#10000218
Phenol Red	Sigma-Aldrich	Cat#P3532
Sodium bicarbonate	aladdin	Cat#S112339
Bafilomycin A1	Selleck	Cat#S1413
Trizol	Sigma-Aldrich	Cat#93289
Sodium 3-trimethylsilyl [2,2,3,3-D4] propionate, TSP	Cambridge Isotope Laboratories	Cat#DLM-48
D_2O	Cambridge Isotope Laboratories	Cat#DLM-7005
		DLM-7005
Trehalase	Megazyme	Cat#E-TREH
Critical commercial assays		
D-glucose assay kit	Megazyme	K-GLUC
MEGAscript T7 High Yield Transcription kit	Thermo Fisher	AMB13345
Accu-Chek Active Blood Glucose Meter	Roche	ACCU-CHEK Active
SYBR Green qPCR Master Mix	Bimake	B21702
5X All-In-One MasterMix	Abm	G492

REAGENT or RESOURCE	SOURCE	IDENTIFIER
Deposited data		
RNA-seq data	This paper	SRA: PRJNA597432
16S rRNA-seq data	This paper	SRA: PRJNA597440
Experimental Models: Organisms/Strains		
Anopheles stephensi	This paper	strain Hor
Anopheles stephensi	JHMRI insectary	strain Liston
Plasmodium berghei	This paper	strain ANKA
Plasmodium falciparum	JHMRI parasitology core	strain NF54
Mouse: BALB/c	Jsj-lab	N/A
Oligonucleotides		
Primers for qPCR: See Table S4	Tsingke	N/A
dsVATPase_H_N3 Forward, GCTCGCTGGACAAGGATAAGAAGG	Tsingke	N/A
dsVATPase_H_N3 Reverse, TCTGGTGATGGTGGCTGTTCG	Tsingke	N/A
dsCaudal Forward, CCGCATCCGCAGTTCATTGG	Tsingke	N/A
dsCaudal Reverse, GCCGCTGTTGGTCCGTGTA	Tsingke	N/A
Asaia1, 5′-AGCACCAGTTTCCCGATGTTAT-3′	Thermo Fisher	N/A
Asaia2, 5′-GAAATACCCATCTCTGGATA-3′	Thermo Fisher	N/A
Software and algorithms		
Rstudio	Rstudio	https://www.rstudio.com/
LightCycler® 96 SW 1.1	Roche	https://diagnostics.roche.com/global/en/products/instruments/lightcycler-96.html
GraphPad Prism 8	GraphPad	https://www.graphpad.com/scientific-software/prism/
SIMCA-P+ 12.0	Umetrics	https://www.sartorius.com/en/products/process-analytical-technology/data-analytics-software/support/knowledge-base/about-simca-p-1201-551246
TOPSPIN 3.0	Bruker Biospin	https://www.bruker.com.cn/en/products-and-solutions/mr/nmr-software/topspin.html
AMIX 3.8.3	Bruker Biospin	https://www.bruker.com.cn/en/products-and-solutions/mr/nmr-software/amix.html
SPSS 16.0	SPSS	https://www.ibm.com/support/pages/downloading-ibm-spss-modeler-160
SAS proc GLM	SAS Institute	https://www.sas.com/en_us/software/university-edition/download-software.html
MATLAB 7.1	Mathworks Inc	https://ww2.mathworks.cn/products.html?s_tid=gn_ps